Irmina Marietheres Pucher, BSc

Monitoring of tablets by spatially resolved NIR-spectroscopy in combination with detailed reference analytics

MASTER'S THESIS

to achieve the university degree of

Diplom-Ingenieurin

Master's degree programme: Technical Chemistry

submitted to

Graz University of Technology

Supervisor

Assoc.Prof. Dipl.-Chem. Dr.rer.nat., Torsten Mayr

Institute of Analytical Chemistry and Food Chemistry

DI. Dr. Patrick Wahl
Research Center Pharmaceutical Engineering

Graz, April 2015

AFFIDAVIT

I declare that I have authored this thesis independently, that I have not used other than the declared sources/resources, and that I have explicitly indicated all material which has been quoted either literally or by content from the sources used. The text document uploaded to TUGRAZonline is identical to the present master‘s thesis dissertation.

Date

Signature

Ich möchte an dieser Stelle meine Dankbarkeit dafür ausdrücken, dass mir die Möglichkeit gegeben wurde diese Diplomarbeit am Research Center Pharmaceutical Engeneering zu verfassen. Durch ihre Unterstützung und kompetenten Ratschläge haben mir die Mitarbeiter des RCPE, besonders das PAT Team sowie die Labortechniker sehr geholfen. Mein besonderer Dank gilt hierbei meinem Betreuer DI. Dr. Patrick Wahl, der mir stets mit Rat und Tat zur Seite stand.

Weiters möchte ich mich bei Univ.-Prof. Dipl.-Chem. Dr.rer.nat. Ingo Klimant und Assoc.Prof. Dipl.-Chem. Dr.rer.nat. Torsten Mayr bedanken, die meine Betreuung seitens der Universität übernommen haben.

Zum Schluss will ich noch meine Eltern und Familie erwähnen, die mich immer bestärkt und unterstützt haben.

Danke!

Table of contents

List of tables

List of figures

List of abbreviations

API	active pharmaceutical ingredient
ATR	attenuated total reflection
ASA	acetylsalicylic acid or aspirin
ff_c	flowability function
FIR	far-infrared
HOMO	highest occupied molecular orbital
HPLC	high performance liquid chromatography
LUMO	lowest unoccupied molecular orbital
MIR	mid-infrared
MO	molecular orbital
MPS	major principal stress
NIR	near-infrared
NIRS	near-infrared spectroscopy
PGP	prism-grating-prism
PLS	partial least squares
UV/Vis	ultraviolet-visible
UYS	unconfined yield strength
wt.%	weight percent

Abstract

The objective of this study was the setup of a chemometric model for the determination of tablet hardness and tablet constituents applying NIR imaging spectroscopy. Reference analytics for the measurement of API content were based on UV/Vis spectroscopy. Tablet crushing strength was analysed using a tablet hardness test instrument.

Samples with different caffeine and aspirin concentrations were manufactured at varying compression force grades using a single punch press. These tablets were then investigated regarding their dissolution properties as well as hardness and API content. The NIR and reference measurement data were evaluated with partial least squares (PLS) regression. Additionally, different lactose samples were tested regarding their rheological properties as well as direct compaction performance.

Zusammenfassung

Das Ziel dieser Arbeit war das Entwickeln eines chemometrischen Modells zur Bestimmung von Tablettenhärte und Inhaltstoffen unter der Anwendung von NIR imaging Spektroskopie. Die Referenzanalytik für die Bestimmung des API Gehaltes basierte auf UV/Vis Spektroskopie. Die Härte der Proben wurde mittels eines Tablettenhärtemessgerätes bestimmt.

Es wurden Proben mit unterschiedlichen Koffein und Aspirin Konzentrationen bei variierender Kompression unter Verwendung einer Tablettenpresse hergestellt. Diese Tabletten wurden dann bezüglich ihres Dissolutionverhaltens, sowie ihrer Härte und API Gehaltes analysiert. Die NIR und Referenz Messdaten wurden mit partial least squares (PLS) Regression ausgewertet. Zusätzlich wurden unterschiedliche Lactose Proben bezüglich ihrer rheologischen Eigenschaften und direkt Verpressbarkeit untersucht.

Introduction

Near-infrared spectroscopy is a fast and non-destructive analytical method that has recently gained a lot of attention in many fields like agriculture or the pharmaceutical industry. One reason for the growing interest in NIR spectroscopy is that for these measurements no sample preparation is required, making it an economically and ecologically rewarding method.

In all kinds of industrial applications product analysis and quality assurance is a very important issue which is why particularly analytical tools, which can be applied in-line, are on demand. NIR is successfully used in process monitoring, product quality assurance and raw material testing. In combination with chemometrics qualitative as well as quantitative analysis is feasible.

A clear advantage of NIR spectroscopy is the possibility to acquire chemical as well as physical information of a specimen at the same time. Therefore, it can not only be applied for chemical identification but also bears information on the physical parameters of the samples under investigation, which can be useful in product quality assurance as well as in process development.

Near-infrared spectroscopy can also be combined with imaging techniques. Chemical imaging enables chemical identification of many compounds simultaneously acquiring spatially located spectra. It is used for the visualization of the chemical compound distribution. This renders it possible to identify the API and the excipients at the same time.

Theoretical Background

1.1. Near-infrared spectroscopy

As a matter of principle spectroscopic analysis is based on physical interactions such as absorbance, transmittance, reflectance, fluorescence, phosphorescence and radioactive decay of atoms or molecules with electromagnetic radiation. These interdependencies bare explicit information about the samples under investigation. The electromagnetic spectrum is generally split in several regions, including gamma- and X-rays, ultraviolet radiation, visible light, infrared radiation, micro and radio waves. Infrared radiation can be further categorized in the regions of near-infrared, mid-infrared and far-infrared.[1,2]

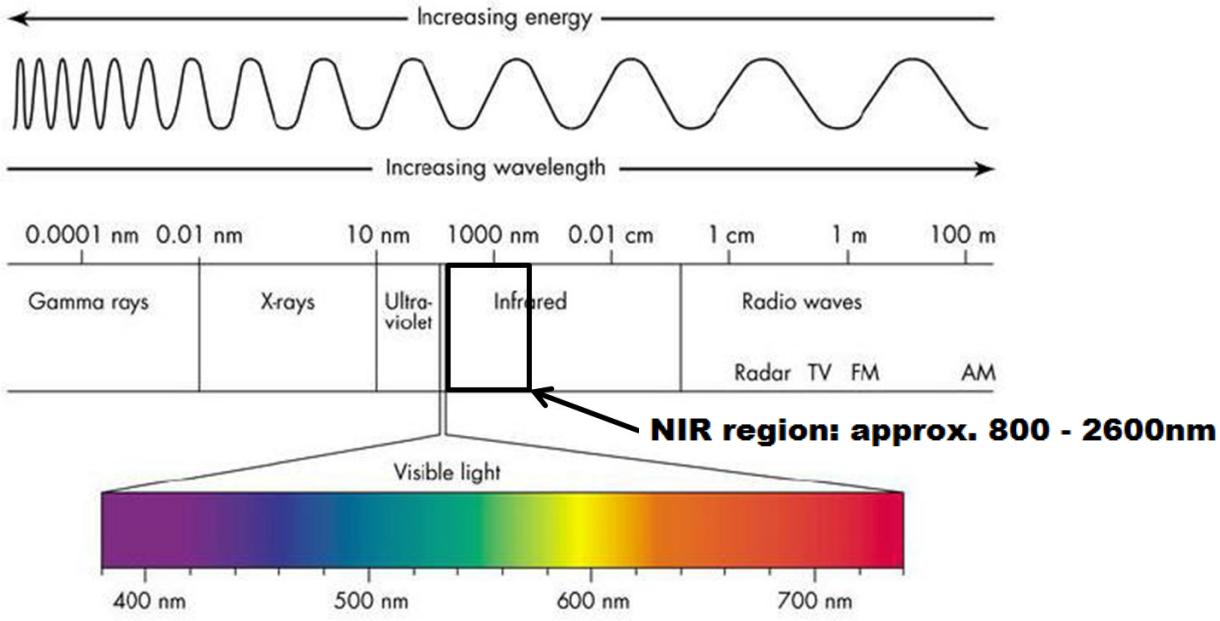

Figure 1: Electromagnetic spectrum with magnified visible spectrum and highlighted near-infrared region (cf.: http://www.scimed.co.uk/nir-spectrometers/).

The area of near-infrared radiation is defined as the region between the visible and the mid-infrared-spectrum and ranges from roughly 800 to 2600nm (12821 to 4000 cm^{-1} respectively). As already mentioned before infrared radiation is subdivided in additional two divisions: far-infrared spanning from 26 to 1000µm (400 to 10cm^{-1}) and mid-infrared representing the region form 2.6 to 26µm (4000 to 400cm^{-1}).[3] Due to their diverse light energy these three sub regions are absorbed by different bonds and molecules. Far-infrared, as the region of least energy is for example absorbed by very heavy atoms like some organometallic or inorganic species while mid-infrared is mostly used in the analysis of organic chemical compounds.[4]

1.1.1. Vibrational spectroscopy

Infrared and Raman are the two main spectroscopic methods based on the detection of molecular vibrational motions. Molecular vibration is described as periodic motion of neighbouring atoms in a molecule. A diatomic molecule represents the simplest case and has only one normal mode of vibration along its bond axis. In polyatomic molecules vibrations are more complex. Every atom has three degrees of motion representing the three space axis resulting in 3N-6 normal modes of vibration in a molecule consisting of N atoms. Linear molecules only exhibit 3N-5 modes of vibration. In general, a distinction between two types of vibrations can be made: vibrations resulting in a change of bond length and vibrations changing the bond angles. Stretching vibrations occur along the bond axis and result in the elongation or shortening of the bond. They can either be symmetric or asymmetric. Vibrations following a change in the bond angles are called deformation vibrations. Molecules can vibrate by twisting, scissoring, rocking or wagging.[1]

Infrared spectroscopy is considered a vibrational technique since the absorption of infrared radiation causes individual bonds to vibrate like a diatomic oscillator.[5] The bond's vibrational frequency is an inherent property which is specific for each chemical bond.[4] In Raman, mid-infrared and near-infrared spectra absorption bands can be observed as a result of molecular vibrations. Due to the sensitivity of the vibrational frequencies to the structure of the chemical compound under investigation, especially MIR spectroscopy is frequently used in the field of structure elucidation. The significant difference between the above mentioned three spectroscopic techniques is that while Raman spectroscopy is regarded a scattering technique, mid-infrared and near-infrared spectroscopy are based on absorption processes. Only distinct frequencies that correlate with the molecular vibrations are absorbed. Therefore, in NIR and MIR applications polychromatic light sources are used, whereas Raman works with monochromatic laser light.[5]

In addition to the change in dipole moment required for infrared-activity, near-infrared spectroscopy also needs vibrating atoms with a large mechanical anharmonicity. It is known that anharmonicity strongly affects the intensity of overtones. Bonds that show low anharmonicity constants are expected to have low overtone intensities. It

appears to be logical that hydrogen bond stretching transitions dominate the overtone spectra since they possess the highest anharmonicity constant values due to the hydrogen atom's low mass. Carbonyl stretching bands show higher overtones with very low intensities due to the fact that these bonds are not as inharmonic.[5]

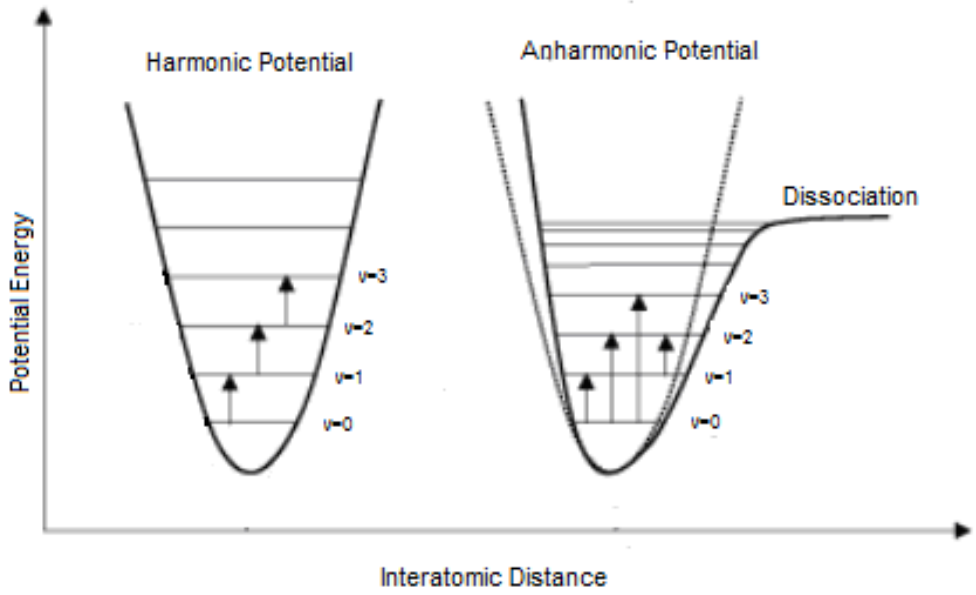

Figure 2: Potential of a harmonic and an anharmonic diatomic oscillator. [Cf.1]

The energy diagram of a harmonic and an anharmonic diatomic oscillator is shown in figure 2. It can be observed that with increasing vibrational states the anharmonic oscillator departs from the perfect parabolic curve shown by the harmonic oscillator. Transitions from v=0 to v=1 are called fundamentals whereas transitions from v=0 to any other energy level different to 1 are called overtones. If an excitation from v=0 to v=2 occurs it is called first overtone, analogically the second overtone is excited from v=0 to v=3. The probability of appearance of overtones decreases drastically with an increase in potential energy. [1]

1.1.2. Principles of near-infrared spectroscopy

Within the near-infrared spectral range mainly overtones and combination bands of functional groups like C-H, O-H, N-H can be observed while overtones representing the most intensive mid-infrared bands rarely exsist.[4,6] This can be explained by the fact that most of the hydrogen bond fundamentals absorb at wavelength numbers greater than 2000cm^{-1} which lets their first overtones arise in the near-infrared range. Overtones of groups absorbing in regions of lower wavelength number can already appear in the mid-infrared region as well. In general overtones are less intense than the corresponding fundamentals. This is why the absorption bands of specific chemical groups are insignificant by the time they reach the NIR region.[5] It is obvious to use near-infrared spectroscopic techniques for the analysis of organic compounds rich in hydrogen bonds. Unfortunately organic compounds contain a vast number of these linkages which results in very complex, not easily interpretable spectra with very broad and overlapping absorption bands.[2,7]

Near-infrared signals are generally 10 to 100 times lower than the corresponding fundamental absorption bands detected in the mid-infrared range because the appearance of combination vibrations and overtones is not very likely. Due to that NIRS does not require any sample preparation and allows adaptation of thicker samples. Another advantage that goes along with the low absorption coefficient is that highly absorbing or scattering specimen can be analysed. [7,3]

1.2. Near-infrared chemical imaging spectroscopy

Since in conventional NIR spectroscopy only point measurements can be conducted sample homogeneity is a very important point concerning the suitability of this technique, especially for solid samples. Inhomogeneity issues can be neglected for liquid and gaseous phase specimen. However, in solid state a lot of information can be lost since spectrometers integrate the whole areal information and therefore only give an insight in the bulk composition of the samples and not in the spatial distribution of the chemical components; thus an imaging technique is required.[2,8]

Imaging spectroscopy is used to generate a spatial map of the spectral information gained from a sample. As its name indicates, this method comprises the advantages of imaging techniques i.e. collect spatial information and spectroscopy. With this technology it is possible to determine the different compounds of a specimen as well as their areal distribution on the sample surface simultaneously. It establishes a three-dimensional dataset, also referred to as hypercube or datacube, from a two-dimensional spatial vector field and a third spectral dimension.[2]

1.2.1. Construction of the datacube

Spectral imaging has been designed to acquire spectral and spatial information from a sample simultaneously. The generated data consists of two spatial dimensions as well as a third one containing the spectral information and maintains chemical and physical information of the material under investigation. These three-dimensional images I (x, y, λ) can either be seen as individual spatial images I (x, y) at every given wavelength (λ) or as spectrum I (λ) at every pixel (x, y). Each of these pixels comprises therefore the spectrum of that specific position which can be used for the characterisation of the sample composition.[2]

There are tree possible ways to built up a spectral image: point-scanning, area-scanning or line-scanning. With the area-scanning method, also called staring mode, images are taken one wavelength after another while the camera's field of view is kept steady. With the point-scanning whisk-broom method a spectrum of a single point is taken. Afterwards the sample has to be moved to record a spectrum at

another position. In the line-scanning or push-broom method spectral information of a line is detected simultaneously by an array detector. Due to its measuring principle this technique is frequently used in conveyor belt applications and has a high importance in industrial applications. Point- and line-scanning methods are considered spatial-scanning modes since the specimen has to be moved either line-by-line or point-by-point while in area-scanning modes the sample does not have to be put in motion at all. Due to this the area-scanning method is also referred to as wavelength-scanning.[2]

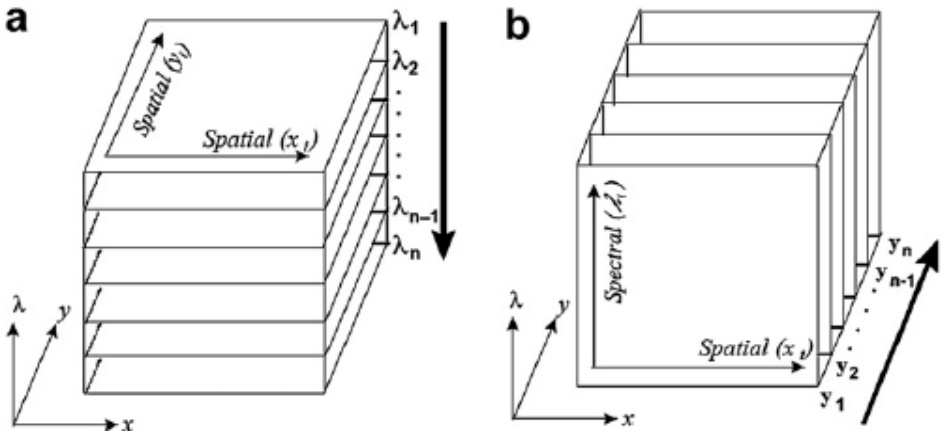

Figure 3: Principle of areal and wavelength-scanning modes.[2]

Figure 3 exemplifies the principle of image acquisition performing areal or wavelength-scanning measurements. Bold arrows illustrate directions for subsequent image acquisition resulting in a hypercube. Image **a** shows a wavelength-scanning mode collecting sequential spectral data. In figure **b** a spatial-scanning system is depicted moving along the y-axis.

1.2.2. Chemometric data processing

Near-infrared spectra generally consist of broad and overlapping absorption bands incorporating physical as well as chemical information of all components present in the sample. Hence the analytical information that can be drawn from these signals is multivariate and scarcely selective. In order to accomplish quantitative or qualitative near-infrared analysis chemometrics have to be applied for reducing “irrelevant” information whilst extracting information relevant for the analysis.[7] The term chemometrics refers to using statistical and mathematical methods for the treatment of quantitative or qualitative data, such as for example spectra, derived from chemical analyses.[6]

Data pretreatments have to be conducted in order to eliminate the spectral parameters resulting from instrumental effects or changing physical sample properties before multivariate models can be applied. In quantitative NIR analysis the most popular multivariate regression methods are partial least squares (PLS) and principal component regression (PCR). These multivariate analysis techniques incorporate the whole quantity of spectral information present in the data cube. Since PLS regression was applied in data analysis this method is briefly described here. The aim of PLS regression is to connect two matrices; the spectral data X with reference data Y. It is applied in forecasting the variables of matrix Y monitoring the variables of matrix X. In order to build up a mathematical model that links the two matrices a calibration is necessary. For this a data set of specimen with known X and Y matrices is required. In NIR chemical compound quantification spectra can be used to create matrix X, while for matrix Y the known concentrations are employed. Before the model can be applied in the analysis of unknown samples it has to be validated using known values.[3]

The analytical target as well as sample properties have an influence on the number of samples that have to be used in a calibration model. The usage of too many data points can lead to so called “overfitted” models. These models often fail validation since they are not robust enough.[7]

1.2.3. Instrumentation

Basically spectral imaging systems consist of three components: a light source, a wavelength dispersion device and a detector.

For spectral imaging mostly photovoltaic semiconductor detectors, also called charge-coupled devices (CCDs) are used. Some of the commonly used detectors consist of silicon (Si), mercury cadmium telluride (HgCdTe), indium antimonide (InSb) and indium gallium arsenide (InGaAs). Depending on their composition these arrays are sensitive in different wavelength ranges. While silicon arrays can be applied in a region from 400 to 1000nm the other afore mentioned arrays are applicable in the area from 1000 to 5000nm. Therefore in some instruments several different - some even overlapping - detectors are used in order to optimize the sensitivity in special wavelength regions.[2] Besides the CCD spectrometers Fourier Transform of FT spectrometers are used frequently. In industrial processes CCD constructions are favoured due to their robustness, rapidity and low prize.

The most popular wavelength dispersion units are built on the basis of diffraction gratings. There are two possible options to build an imaging spectrograph; either using a transmission or a reflection grating.[9]

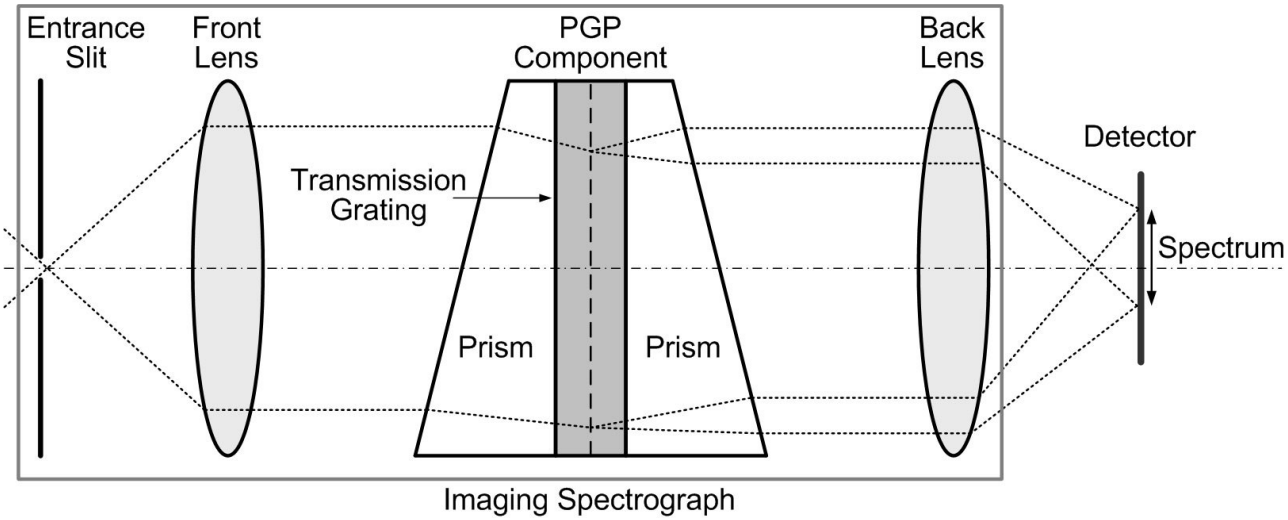

Figure 4: Operating principle of a PGP (prism-grating-prism) imaging spectrograph.[9]

Figure 4 depicts an imaging spectrograph using a transmission grating. The working principle of the shown spectrograph depends on a Prism-grating-prism (PGP) arrangement. The objective lens focuses the light onto the entrance slit. The

incoming light is then collimated by the front lens, dispersed by the grating and focussed by the back lens on the detector array. The incoming light is dispersed by the grating into different wavelength preserving spatial information. This results in a two-dimensional image where one dimension represents the spectral and the other the spatial information of the scanning line.[9] The required third dimension for the generation of a hypercube i.e. the second spatial dimension is set up by moving the camera's field of view i.e. moving the sample.[2]

There are different ways of measuring interactions of the sample with the light emitted by the source. If the transmitted light has to be recorded the detector is placed behind the illuminated sample.[3] Transmission measurements are commonly conducted for thin samples but can be applied in the analysis of thick specimen like tablets as well. These analyses take more time and therefore cannot be used for fast chemical imaging. Still, this method is common in at-line tablet analyzers which can also measure physical parameters like hardness, thickness, diameter and weight. In order to record the reflected light the detector is placed on the same side as the source illuminating the specimen. For this test the sample has to be assumed of infinite thickness and therefore incapable of transmission. In chemical imaging analysis of pharmaceutical solid dosage forms mostly diffuse reflectance systems are used. In these tests the light is scattered by the sample particles and a fraction of the radiation is then reflected by the sample and can be recorded by the detector. Especially near-infrared diffuse reflectance methods are often applied in the image analysis of opaque or thick specimen in pharmaceutical as well as food industry applications. For classical mid-infrared single point measurements ATR is frequently applied, since it was developed in order to eliminate sample dilution which is not necessary in near-infrared measurements because the bands are relatively weak in comparison to the MIR range.[3]

1.2.4. Advantages and disadvantages of NIR spectral imaging

Comparing spectral imaging with other spectroscopic methods reveals some striking advantages but demerits as well. In imaging spectroscopy there is no sample pre-treatment or preparation necessary. Its non-destructive and non-invasive nature offers the opportunity to analyse the whole batch rather than just performing spot tests by thief sampling which would have to be conducted with destructive methods. Since the samples´ chemical compositions are determined it is possible to sort them regarding their chemical constituents. For some industries this is of particular importance because divergent qualities can be prized differently. Furthermore, customer preferences as well as market requirements can be labelled. Still in pharmaceutical applications it should be the main aim to reach product specifications. Additionally, near-infrared spectroscopic imaging is a chemical-free test which renders it a save and environmentally friendly analytical approach considering that there are no solvents or harmful reagents involved in sample preparation. These characteristics make it also very interesting regarding economics. Due to its chemical-free nature waste treatment costs and reagent costs can be saved. Another advantage is that a spectrum for each pixel on a specimen is collected, not only one spectrum at a single spot. Several constituents can be determined simultaneously as well as their spatial distribution and concentration while other analytical methods can only give an insight in the bulk composition of the sample. Chemical imaging is used to generate maps of a sample's surface composition. It visualizes various chemical components in a sample on the basis of their spectral properties since regions of identical chemical composition should exhibit the same spectral signature.[2]

Still imaging spectroscopy has some demerits that have to be discussed as well. It generates a comprehensive quantity of data which is computationally intensive as there is some redundant information included as well. For the analysis of this vast amount of information the utilization of chemometrics is necessary. A limiting factor especially in industrial applications is the hardware speed required for fast image acquisition and data analysis. Due to the amount of overlapping bands near-infrared spectra are difficult to interpret since the individual bands can not be accurately allocated to the corresponding chemical groups. Furthermore, the concentration of

the chemical compound needs to reach a minimum value in order to be detectable. Another challenging aspect is that the spectra are influenced by physical and chemical effects such as pressure, temperature or particle size distribution. As the power of hyperspectal imaging technology lies in resolving inhomogeneous samples spatially, this technique is not reasonable for the analysis of liquids and homogenous samples since a convenient single point spectrometer is capable of generating the identical spectral information.[2]

1.2.5. Applications of NIR spectroscopy

Combined with chemometrics near-infrared spectroscopy has become very important for qualitative and quantitative analysis in pharmaceutical industry applications as well as other fields like food industry or agriculture. It is very often the method of choice since it is non-destructive, economic and very rapid. NIR-spectroscopy can be applied in the analysis of solids, liquids and gases. This technique can be carried out in development, process monitoring in industrial production as well as for quality conformance tests in analytical control laboratories.[6]

Moisture determination has been one of the first implementations for NIR analysis in the pharmaceutical industry. Water content is a critical factor speaking of long term and microbiological stability.[6] Water can easily be detected due to two strong absorbing bands located around 1450nm and 1940nm. A very important advantage of near-infrared spectroscopy in this context is that it can also be applied on lyophilised products to diagnose the moisture content very rapidly even through intact glass vials without having to open them risking contaminations because glass is transparent to NIR radiation since it possesses no significant hydrogen bonds.[3,6] Not only water can be detected by near-infrared spectroscopy but also other residual solvents like methanol or ethanol.[4]

Blending processes are crucial especially in manufacturing solid dosage forms. Without proper blending, it is virtually impossible to reach an output with the required API content. Therefore, a homogenous blend should always be aspired. Identification of a homogeneous blend by analytical methods such as HPLC or UV/Vis

spectroscopy might be fault-prone because samples are taken from the blender with a sample thief. Furthermore, with these chemical methods only the API distribution is determined. Although it is not possible to draw conclusions considering the blend only by investigating the API content it is assumed that the excipients are as homogeneously distributed as the API. In comparison to NIR spectroscopy the used chemical analyses are costly, destructive and time consuming as they are conducted off-line. Another advantage of near-infrared analysis regarding powder blend homogeneity is the possibility to monitor all components, not only the API distribution. On-line as well as in-line application of near-infrared spectroscopy is feasible because it is neither destructive nor invasive and fast enough for real time measurements.[3,6] Still, for NIR measurements reference analytics like HPLC or UV/Vis are essential as it is only a secondary analytical method.

Another important scope of application in the pharmaceutical industry is the use in granulation. In many processes powder blending is followed by either wet or dry granulation. These granulates are often further processed in tablet compression, are used as capsules filling or are the final drug form themselves. Moisture is a critical parameter in granulation influencing the granules growth kinetics as well as the solid-state characteristics of the granules and therefore the final dosage form's properties.[6] Near-infrared spectra do not only hold information about the chemical, but also the physical attributes of solid samples. Amongst these physical parameters are dissolution rate, particle size, compaction force, tablet porosity, tablet hardness and crushing strength.[6,,10] Most publications referring to the application of near-infrared spectroscopy in determining tablet hardness or crushing strength indicate that increasing tablet hardness leads to an increase in NIR absorption due to the smoother tablet surface.[10] NIRS has also successfully been applied in the characterisation of polymorphism, the ability of a solid to appear in different crystalline forms. This can have a strong impact on the dissolution properties or the stability of a solid dosage form.[6]

Depending on the plastic material used tablets can be identified even through blister packaging. [3,7]

1.3. Dissolution testing

This test is used for the analysis of solid oral dosage forms like for example tablets or capsules, in order to monitor the dissolution properties of their active ingredients and to ensure they meet the requirements set.[11,12]

The API has to be absorbed by the body and transported to its active site. Therefore, the bioavailability of a drug substance is very important for its efficiency. Generally bioavailability is described by dissolution and absorption properties. The term dissolution describes the drug substance's extraction of the solid matrix in the gastrointestinal tract. Absorption defines the transport process into the systemic circulation from the gastrointestinal tract. In vitro laboratory dissolution tests were designed to give an insight in the extraction process of the active ingredient out of the dosage form matrix. Still, only conclusions regarding in vivo dissolution can be drawn from these in vitro tests. It is not suitable for the investigation of bioavailability since it provides no information about in vivo absorption of the drug substance used in the test. Nevertheless, these tests gather important data about the properties of the solid dosage forms as they primarily depend on product formulation and the production parameters. Dissolution tests are used in the development of drug formulations and as quality assurance tests in industrial applications for batch to batch consistency tests.[13]

While developing a dissolution methodology the drug substance's solid state properties have to be considered since they can have a strong impact on the active pharmaceutical ingredient's dissolution behaviour. Other important parameters like the type of dosage form, compaction strength and release mechanism also have to be kept in mind. Water is generally not considered a suitable medium due to its variability in pH and ionic strength. Normally 1N hydrochloric acid, acetate or phosphate buffers are used as medium. To enhance the drug solubility surfactants can be added to the solutions. For some tests a change in the medium's pH-value is necessary to simulate the desired in vivo dissolution process. At first an acidic solution is used representing the stomach which is followed by an alkaline medium like it can be found in the intestine.[13]

For the analysis of the dissolution samples mostly UV/Vis spectroscopy or high performance liquid chromatography (HPLC) is applied.[13]

Figure 5: ERWEKA dissolution tester DT 820 Series.

For dissolution tests the paddle apparatus, in US Pharmacopeia also called Apparatus 2, was employed. The mentioned paddle consist of a shaft and a blade which are inert by themselves or are coated with a material that is inert to prevent the parts of the apparatus from interfering with either the dissolution medium or the preparation. During the test the dosage unit is not allowed to float. Sinkers can be used to prevent the tablets or capsules from floating. [11,12]

1.4. Ultraviolet-visible spectroscopy

The term ultraviolet-visible (UV/Vis) spectroscopy refers to reflectance or absorption spectroscopy in the regions of ultraviolet and visible light. The range of visible light spans roughly from 400 to 750nm. Ultraviolet radiation reaches from 400 to 10nm and is subdivided in UV-A, UV-B and UV-C radiation due to their diverse biological impact. [14] UV/Vis spectroscopy is usually only applied in spectral ranges going down to a minimum of 200nm. Within this region quartz glass starts to absorb. Additionally at wavelength shorter than 200nm atmospheric gases present in air show significant absorption. Therefore, experiments within this region have to be conducted in inert atmosphere or under vacuum which is why this radiation is commonly referred to as vacuum-UV.

If a photon is striking a molecule without ionization the absorbed amount of energy can principally provoke three changes. Electrons can either be excited to higher energy states, or molecular vibration or rotation increases. In the visible and ultraviolet region of electromagnetic radiation the electronic share in absorption is much bigger then the vibrational and rotational proportion. Long-wave infrared radiation with a wavelength greater than 800nm primarily uses its energy for inducing rotation and vibration. On the contrary absorption in the UV/Vis region with wave length below 800nm provokes the excitation of valence electrons. Additionally slight vibration and rotation processes are activated. If the photon's energy absorbed by the molecule equals the energy difference between an occupied and an unoccupied orbital it can be used to lift an electron to the unoccupied orbital. The electron can then return to its ground state by emission processes like fluorescence or phosphorescence. In this context two molecular orbitals are of particular importance: the highest occupied molecular orbital (HOMO) and the lowest unoccupied molecular orbital (LUMO). Since the energy difference between these two orbitals is the least and electron transitions are most likely. [15]

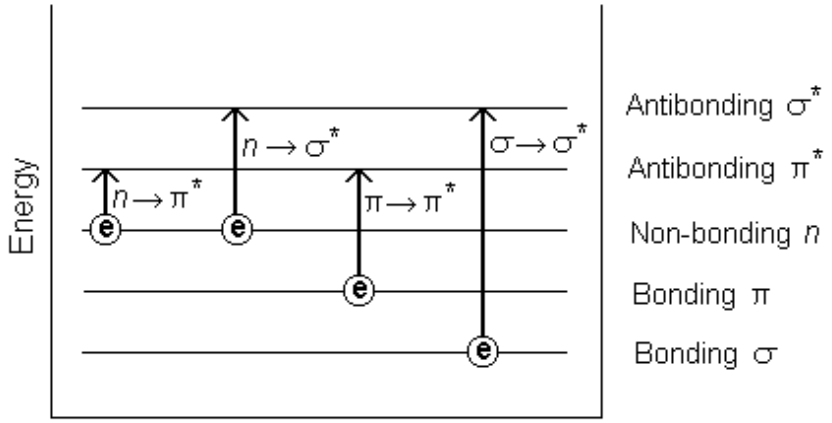

Figure 6: Electronic transitions in molecular orbitals. [Cf 15]

In molecules we distinguish between three different types of electrons. σ-electrons form single bonds (σ-bonds) while π-electrons can be found in multiple bonds (π-bonds). Electrons that are bound to a heteroatom as lone pair are called n-electrons or non-binding electrons. In the molecular orbital theory all atomic orbitals are transformed in bonding and anti-bonding (marked with *) molecular orbitals. As it can be seen in figure 6 the σ→σ* transition is the most energy-intensive and therefore only can be performed with very short wave length. Hence this transition is not of a high importance in ultraviolet-visible spectroscopy. π→π* and n→π* transitions are the most relevant in UV/Vis spectroscopy. These transitions are very important in the analysis of unsaturated hydrocarbons and carbonyl compounds.[15]

Light with a certain intensity I_0 is used for the analysis of a medium with absorbing molecules dissolved. After passing through the cuvette the light shows a different intensity I. Transmission is defined as the quotient of these two intensities.

$$T = \frac{I}{I_0}$$

T is the transmission, I_0 the intensity of incident radiation and I the intensity of the radiation transmitted. The negative decadic logarithm of transmission is called absorption and is defined by the Beer-Lambert-law as follows

$$A = -\log\frac{I}{I_0} = \varepsilon \cdot c \cdot d$$

Where A stands for the absorbance, ε is the molar decadic extinction coefficient, c the concentration in the medium and d the layer thickness. Absorbance and transmission depend on the layer thickness of the absorbing material.

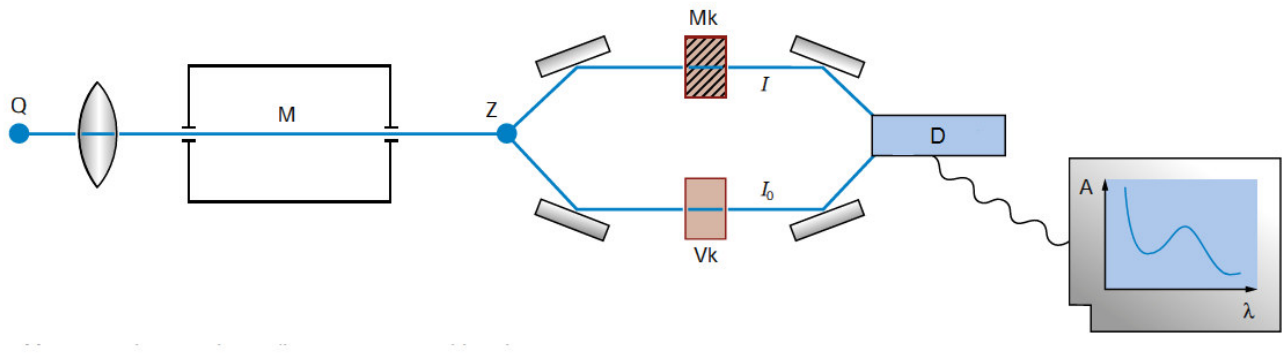

Figure 7: Schematic construction of a UV/Vis double-beam spectrophotometer.[14]

There are two types of spectrophotometers used in UV/Vis spectroscopy: single-beam and double-beam. Single-beam spectrophotometers represent the earliest models and are still in use for some applications. Unlike single-beam, where all of the light passes through the cell, double-beam constructions split the light into two separate rays. One of these beams is used for reference measurements while the other is used for investigating the sample. Reference data is subtracted form sample data and the ratio represents the measurement displayed. Figure 7 illustrates the schematic construction of such a double-beam spectrophotometer where Q represents the radiation source. For the ultraviolet region often hydrogen or deuterium lamps are used while in the visible region tungsten filaments are employed. A monochromator M consisting of a prism or a diffraction grating is applied for spectral dispersion. Z is the point where the light beam is split as explained before. The two beams are then passing through the reference cuvette Vk which is filled with pure solvent and the sample cuvette Mk. The detector D processes the data and afterwards the final spectrum is displayed. [14]

1.5. Rheology

Powder Rheology is particularly important in industrial applications since it can explain the powders behaviour in production processes. It helps in the development of suitable formulations for special industrial plats and renders it possible to compare different materials based on measurable parameters.

Powder shear characteristics allow conclusions pertaining to the flowability of a consolidated powder. This is of special importance since during storage as well as in industrial processing powders often undergo consolidation processes. In order to induce flow the powder's yield point has to be overcome. This point is strongly affected by physical qualities like size, shape and surface properties of the particles. Moisture also has a crucial impact on the flow properties of powders and therefore has to be considered in industrial applications too. For the tests a FT4 powder rheometer from Freeman Technology with a 1ml shear cell module, as pictured in figure 8, was used. It consist of a shear head inducing both rotational and vertical stress on the sample and a vessel filled with powder. The shear head induces a normal stress by moving downwards until it comes into contact with the powder. Then the head begins to rotate promoting shear stress and creating a shear plane right below the blades mounted on the shear head. Throughout the test shear stress is increased while normal stress is kept constant. The point with maximum shear stress, also called yield point or point of incipient failure, is reached as soon as the powder bed no longer resists the shear cell movement and fails or shears. [a]

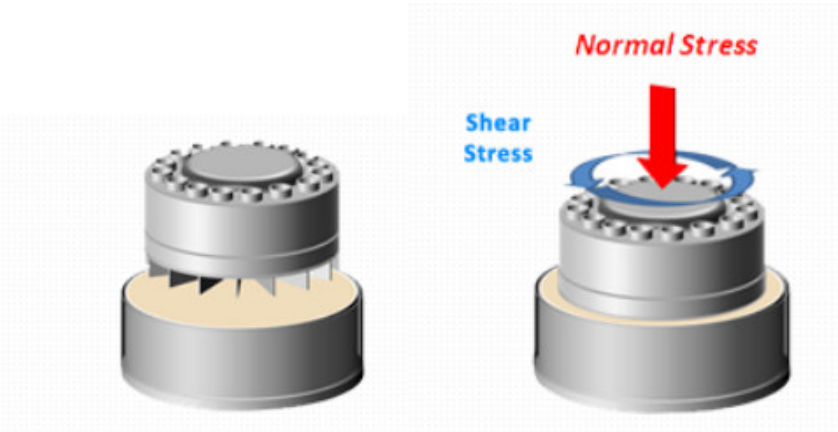

Figure 8: Shear head module used for the test. [a]

[a] Cf. Freeman Technology product information.

Experimental Part

2.1. Chemicals

Lactose:

The Lactose samples used for the tests were all purchased from Meggle.

Tablettose100	Art:4005; Ch Nr: 1414
Tablettose70	Art:4152; Ch Nr: 1405
InhaLac70	Art:9860; Ch Nr: 1342
InhaLac120	Art:4094; Ch Nr: L151462
GranuLac70	Art:4152; Ch Nr: 1405
GranuLac140	Art:4142; Ch Nr: 1414
GranuLac200	Art:4152; Ch Nr: 1405
SpheroLac100	Art:4132; Ch Nr: 1407

Caffeine:

Caffeine purum anhydrous >90% purchased from Sigma Aldrich (Nr: 27600);
Fluka 500g, P.code: 101150644.

Kollidon:

Kollidon CL-M; Crospovidone Ph. Eur., Typ B, purchased from BASF
2kg, Art: 50371464; Ch Nr: 57982224040
Kollidon 30; Povidone K30 Ph. Eur., purchased from BASF
5kg, Art: S10445; Ch Nr: 40595656PO

Magnesium stearate:

Magnesium stearate pure Ph. Eur. purchased from Applichem Panreac;
10kg, Ch Nr: 4R013980

Aerosil:

Aerosil 200 VV Pharma purchased from Evonik; AE 01002, Ch Nr: 13/0040

Hydrochloric Acid:

Rotipuran 37%, p.a., ISO, max. 0,005 ppm Hg purchased from Roth
1l, Art: X942.1; Ch Nr: 194214049

Acetylsalicylic Acid:

ASA Ph. Eur.; Rhodine 3080; 2.5kg donated by GL Pharma

2.2. Rheological Tests

All lactose samples were tested regarding their shear properties using a FT4 powder rheometer from Freeman Technology. The measurements were carried out in a 1ml shear cell at applied normal stress values between 3kPa and 1kPa at 22°C and a relative humidity of 65.0%. The powders were not desiccated to ensure conditions similar to those in production. The samples were filled into the vessels and in a first step conditioned using a blade. Afterwards a vented piston was applied for pre-consolidating the sample. The benefit of this step is that entrained air can be removed easily. Additionally pre-consolidation prevents excess powder from manipulating the measurements. Subsequently the sample was split and the shear cell head applied for reconsolidation of the sample. [a]

Before every shear test a pre-shear was undertaken for conditioning the sample in order to generate reliable and repeatable results. At every point of incipient failure the normal stress and shear stress were registered and plotted on a graph. Three measurements were conducted for every sample, their yield loci values were then averaged and the resulting graphs are shown in figure 9 where shear stress is plotted against target normal stress.

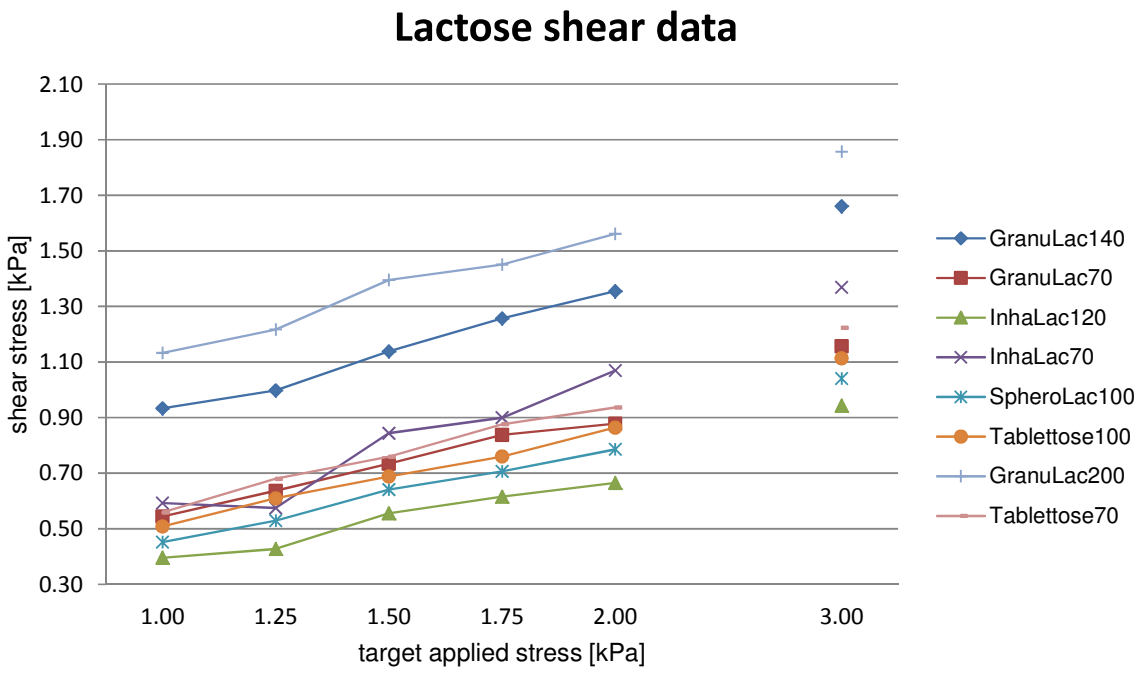

Figure 9: Lactose yield loci.

Additionally cohesion, unconfined yield strength, major principal stress and flowability function values have been determined for all the powders used in the shear tests. The flowability function ff_c can be calculated using the following equation

$$ff_c = \frac{\sigma_1}{\sigma_c}$$

where σ_1 stands for major principle stress and σ_c for unconfined yield strength. Major principle stress is defined as the maximum normal stress applied on a sample. Unconfined yield strength is the stress required for a consolidated sample to fail. Therefore to induce flow the applied stress has to be greater than σ_c.

The larger the ff_c values the better the solids flow properties are. Based on the classification according to Jenike shown below the sample's ease of flow was characterised.

$ff_c < 1$	not flowing
$1 < ff_c < 2$	very cohesive
$2 < ff_c < 4$	cohesive
$4 < ff_c < 10$	easy-flowing
$10 < ff_c$	free-flowing

Table 1: Cohesion, unconfined yield strength, major principle stress and flowability function values of all lactose powders tested.

	Cohesion [kPa]	UYS [kPa]	MPS [kPa]	ff_c
GranuLac200	0.47	1.59	4.83	3.08
GranuLac140	0.36	1.17	4.60	3.94
GranuLac70	0.23	0.63	4.07	6.42
InhaLac120	0.13	0.35	3.89	11.29
InhaLac70	0.17	0.51	4.31	8.71
SpheroLac100	0.18	0.48	3.97	8.33
Tablettose100	0.20	0.55	4.02	7.60
Tabettose70	0.24	0.67	4.23	6.67

As can be obtained from table 1 none of the used samples is not flowing or shows very cohesive properties. GranuLac200 and GranuLac140 are cohesive powders, while GranuLac70 as well as InhaLac70, SpheroLac100 and both Tablettose70 and Tablettose100 are easy-flowing. With an ff_c value greater than 10 only InhaLac120 can be considered free-flowing.

Generally speaking, powders with high shear stress show poor flowability and are prone to be problematic in processes. The lactose samples used in the tests were produced in different processes leading to particles of different size and shape. The great impact of production processes on the flowability of powders can be observed examining the lactose sample's performance during the shear tests.

In comparison to the other lactose samples GranuLac200 and GranuLac140 show distinctly higher shear stress. The product name GranuLac describes recrystallized α-lactose monohydrate that has been further processed by milling. Milling usually results in fine, sharp-edged particles with cohesive powder properties. This type of lactose is often used in wet and dry granulation processes. GranuLac200 has the highest shear stress since it consists of the smallest particles. The smaller the particles, the higher the surface area and the more likely interparticular interactions are. If the surface area to volume ratio is large the interparticular forces are stronger than the body forces. These interactions are also the reason for the cohesive behaviour of GanuLac200 and Granulac140. Due to its larger particles GranuLac70 does not have such a high cohesion. GranuLac70 shows quite similar shear properties, cohesion and flowability as Tablettose70 and Tablettose100. SpheroLac100 is a sieved α-lactose monohydrate with a very good powder flow. InhaLac is applied in dry powder inhalers for pulmonary and nasal drug delivery. It is produced by crystallization and subsequent sieving steps. Theses powders mainly consist of coarse tomahawk-shaped single crystals with only a few agglomerates. Coarser fractions exhibit a higher proportion of agglomerates. Generally the sieved samples have the highest flowability function values. InhaLac120 shows the least shear stress and the highest flowability function of all lactose samples tested. Tablettose70 and Tablettose100 are agglomerated lactose samples which combine the good flow properties of coarse with the sound compactibility of fine milled particles. Tablettose is produced in a process where fluidized fine milled particles are soaked with a binder. They form agglomerates by building liquid bridges that persist after evaporating the binder. These agglomerates have a nearly spherical shape with a very rough and highly structured surface often referred to as popcorn or blackberry structure.[b]

[b] Cf. Meggle product specifications.

2.3. Compaction tests

All lactose samples were tested regarding their direct compaction properties using the Stylcam 200R direct compactor from Medel Pharm. Not all lactose samples are suitable for direct compression processes. Sometimes they have to be modified to reach the required high powder flow and compressibility necessary to perform satisfactory in direct compaction. A powder's compressibility depends on its surface area and the fragmentation occurring during the compaction process.

At first pure Lactose tablets were produced applying a compression force of 20kN. As expected Tablettose70 and Tablettose100 showed very good direct compaction characteristics since these powders are designed for this purpose. InhaLac70 also delivered good results while InhaLac120 tablets adhered to the press and split laterally. This is also called capping and occurs due to air entrapped in the compact. The tablets produced from SpheroLac100 also stuck to the press and decomposed in layers without additional pressure. The tested GranuLac samples showed bad direct compaction properties. Granulac70 tablets also stuck to the press and fragmented in layers on the hardness test. Due to their cohesive behaviour and resulting bad flowability GranuLac140 and GranuLac200 were not easy to feed which resulted in inconstant filling and therefore inconsistent compaction forces and tablets with very unevenly spread thickness and mass. Generally the binding capacity of a powder increases with increasing surface area because the interparticular interactions are higher. Therefore small particles should have good compactibility since they possess favourable dry binding properties. Unfortunately these small particles have poor powder flow properties which make milled α-lactose monohydrate, like GranuLac, improper for direct compaction applications.

In order to improve the direct compaction properties and the powder flowability excipients were mixed with the lactose samples. The excipients added were magnesium stearate which should act as a lubricant and the flow additive Aerosil. Especially when magnesium stearate is used particle fragmentation during compaction is very important since new surfaces are generated which are not covered with the lubricant and therefore have good binding properties.

InhaLac120 and GranuLac70 were mixed with 1wt.% magnesium stearate to prevent the generated tablets from sticking to the press. The other GranuLac samples as well as SpheroLac100 were immingled with 1wt.% magnesium stearate and 1wt.% Aerosil to improve their powder flow properties as well. Inhalac120, GranuLac70 and SperoLac100 tablets no longer adhered to the press and provided good compacts. Though Granulac140 and Ganulac200 were not satisfactorily compactable and did not show constant compression forces. Still, the compaction force values had a narrower distribution in comparison to the pure lactose tablets.

In order to generate representative and reproducible data GranuLac200 was replaced by Tablettose70 as a model substance due to the findings made in the compaction tests and rheological investigations. GranuLac200 is a comparatively cohesive powder and shows poor flowability in comparison to Tablettose70. Feeding was challenging resulting in variations in die filling and therefore compaction force. Even with additional flow additive and lubricant it had a very bad performance resulting in inconstant tablet mass and thickness. Tablettose70 on the other hand could be fed without any problems and performed well in the direct compaction tests.

Although all tablets were produced at constant filling height they had very different thickness and mass. Depending on the number of tablets produced between seven and eighteen flawless samples were weight and their thickness and diameter measured. The averaged values can be found in the following chart. It was not possible to determine the physical dimensions of pure GranuLac200 tablets because direct compression was not successful at all.

Table 2: Physical dimensions of the lactose tablets produced.

	Excipients [1%wt]	h [mm]	d [mm]	m [mg]
GranuLac200		-	-	-
	Mg-stearate, Aerosil	3.30	12.06	492.3
GranuLac140		3.34	12.01	474.2
	Mg-stearate, Aerosil	3.69	12.05	560.1
GranuLac70		4.22	12.03	628.8
	Mg-stearate	5.19	12.07	807.2
InhaLac120		4.44	12.04	659.3
	Mg-stearate	4.89	12.07	756.4
InhaLac70		3.82	12.06	574.4
SpheroLac100		4.47	12.09	632.9
	Mg-stearate, Aerosil	4.53	12.07	695.6
Tablettose100		3.48	12.07	505.1
Tabettose70		3.53	12.04	508.7

Especially GranuLac70, InhaLac120 and SpheroLac100 resulted in very thick tablets while InhaLac70, Tablettose70 and Tablettose100 are considerably thin. With the addition of Aerosil the tablet mass as well as their thickness increased indicating a better flow. The tablets with lubricant added also had a neat surface and increasing values in thickness and mass since they were no longer sticking to the press and could be removed as a whole. Comparing tablets produced from the different GranuLac lactose powders it can be observed that tablet thickness and mass increase with increasing particle size, which again reflects the cohesive properties and poor flowability of powders with small particles.

Table 3: Tablet's crushing strength values and standard deviation.

	Excipients [1%wt]	Crushing strength [N]	SD [N]
GranuLac200		-	-
	Mg-stearate, Aerosil	-	-
GranuLac140		-	-
	Mg-stearate, Aerosil	-	-
GranuLac70		58.90	15.32
	Mg-stearate	35.07	3.33
InhaLac120		77.93	9.25
	Mg-stearate	38.73	2.42
InhaLac70		59.77	3.02
SpheroLac100		46.30	20.74
	Mg-stearate, Aerosil	54.43	2.55
Tablettose100		72.43	11.10
Tabettose70		35.03	8.34

Tablets were then analyzed using the tablet hardness testing instrument 311E from Pharma Test. Between five and seven tablets for every sample were used for determining the average crushing strength.

GranuLac200 and GranuLac140 samples were not examined since the force during compaction as well as the tablets mass and thickness varied too much to generate representative data. With the addition of excipients the standard deviation could be highly reduced which leads to the conclusion that the flow during feeding could successfully be improved and therefore compaction forces are not varying that intensely anymore.

2.4. Tablet fabrication

2.4.1. Aspirin tablets

Mixtures with an API content of 8wt.%, 9wt.%, 10wt.%, 11wt.% and 12wt.% were produced from acetylsalicylic acid and Tablettose70. They were blended for 15 min with a Turbula mixer type T2F System Schwartz from Willy A. Bachofen AG. As lubricant 1%wt magnesium stearate was added to the mixture. Tablets were then produced with the Stylcam 200R direct compactor at a speed of 2.5 tablets per minute and a filling height of 7.4mm applying compression forces of 5kN, 10kN, 15kN, 20kN and 25kN.

The tablet's crushing strength was determined for all API concentrations at every compaction force with the tablet hardness testing instrument. The values for all aspirin concentrations showed the same trend as can be seen in figure 10. However, the highest and lowest API concentration's results at 25kN vary strongly.

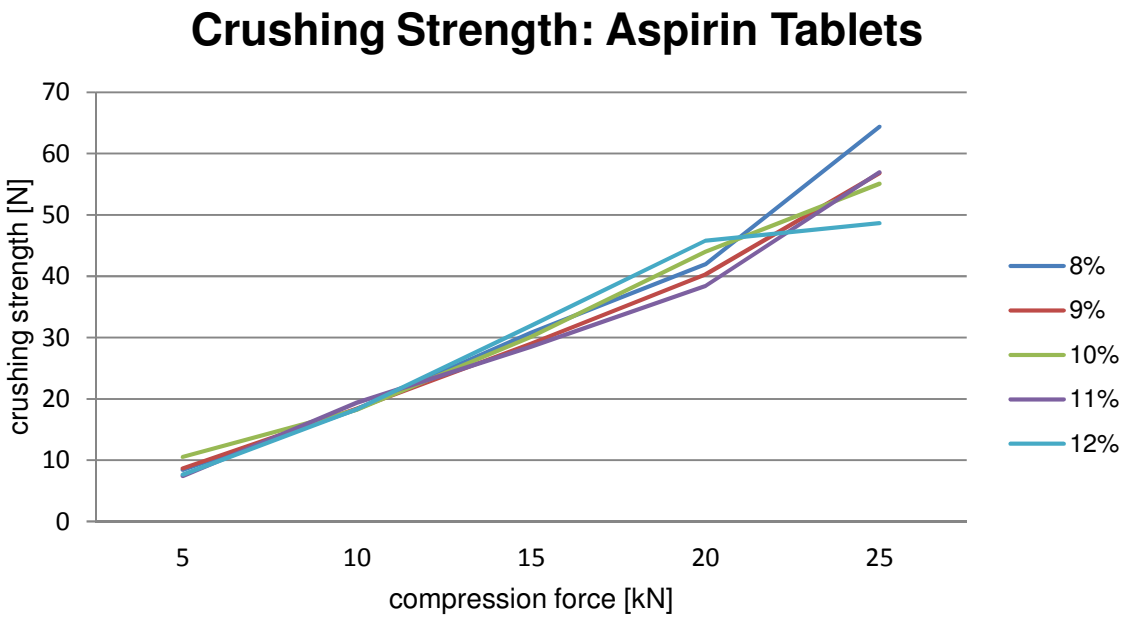

Figure 10: Aspirin tablet's crushing strength values.

Table 4: Aspirin tablet's crushing strength values.

	Crushing strength [N]				
Compaction force [kN]	8wt.%	9wt.%	10wt.%	11wt.%	12wt.%
5	8.43	8.63	10.52	7.40	7.63
10	18.28	18.43	18.23	19.38	18.28
15	30.80	29.02	30.12	28.52	31.93
20	41.95	40.30	44.00	38.40	45.80
25	64.43	56.82	55.08	56.96	48.65

Table 4 presents the averaged crushing strength values used in figure 10. No significant difference between the API concentrations can be observed. Aspirin tablets are generally rather soft. They are easily dented and rather deform than fracture during the hardness test as well as when dropped.

Additionally the tablet's mass and thickness were investigated. They had an average mass between 0.55g and 0.58g. These masses were used for calculating the theoretical maximum and minimum API concentration in a tablet. As expected it could be observed that the tablet's height decreased with increasing compaction force from 4.2mm at a compaction force of 5kN to 3.8mm at 25kN.

2.4.2. Caffeine tablets

Powder mixtures with an API concentration of 4wt.%, 4.5wt.%, 5wt.%, 5.5wt.% and 6wt.% were produced from Tablettose70 and caffeine adding 5wt.% Kollidon CL-M. In order to prevent the tablets from sticking to the press again 1wt.% magnesium stearate was admixed. The powders were also blended for 15min on the Turbula mixer. Tablets were then manufactured at a speed of 2.5 tablets per minute and a filling height of 7.42mm with the Stylcam 200R direct compactor at the following compaction forces: 5kN, 10kN, 15kN, 20kN, 25kN and 30kN.

Again crushing strength was examined for all API concentrations at every compaction force. As expected crushing strength increases with increasing compression force. All of the mixtures show a quite similar trend. For an unknown reason the values determined at 5wt.% are lower than the others as can also be seen in table 5.

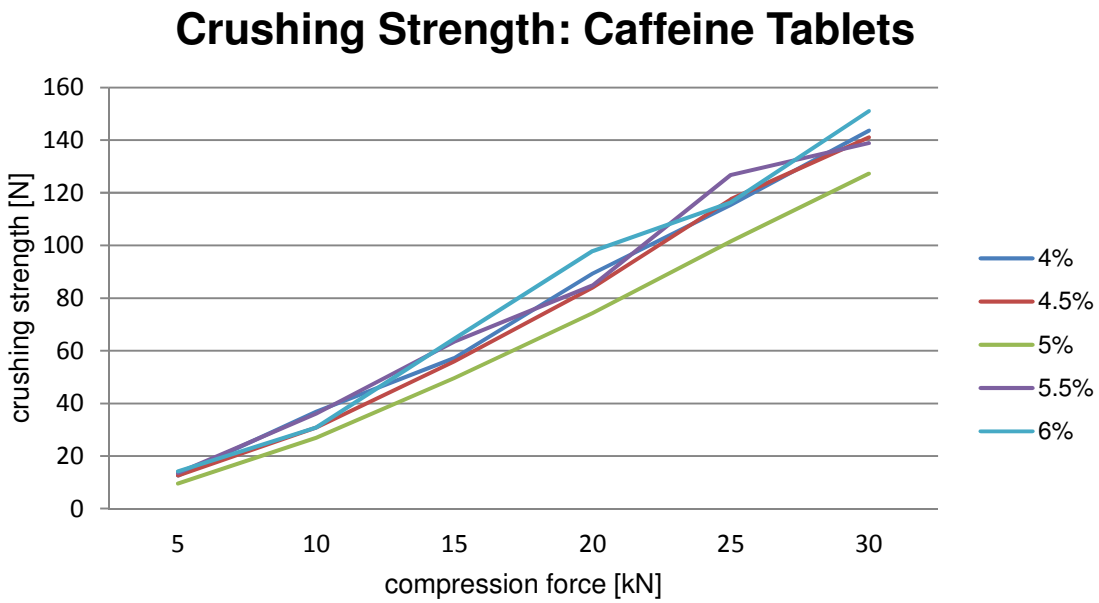

Figure 11: Caffeine tablet's crushing strength values.

Table 5: Caffeine tablet's crushing strength values.

	Crushing strength [N]				
Compaction force [kN]	4wt.%	4.5wt.%	5wt.%	5.5wt.%	6wt.%
5	12.63	12.60	9.50	13.53	14.17
10	36.83	30.77	26.87	36.13	30.83
15	57.23	55.90	49.63	63.50	64.57
20	89.34	83.97	74.28	84.85	97.87
25	115.44	117.53	101.55	126.80	116.32
30	143.63	141.07	127.28	138.90	151.13

The tablet's physical dimensions were also investigated. Again tablet thickness decreased with increasing compaction force from 4.4mm at a compression force of 5kN to 3.6mm at 30kN. No striking variation between the different API concentrations could be observed. The tablets had an average mass between 0.55g and 0.57g. These average masses were, analogous to the ASA tablets, used for calculating the tablet's theoretical maximum and minimum API concentration.

Aspirin tablets have a much lower crushing strength then caffeine tablets produced at the same compression force. Caffeine tablets manufactured at 20kN and 25kN are about twice as hard as the corresponding acetylsalicylic acid tablets. This can be explained by the higher API concentration present in the aspirin tablets which leads to a greater impact of the API on the powder mixture's properties. Caffeine and aspirin have totally different particle morphology. While the caffeine powder used consists of granulated particles the acetylsalicylic acid crystals are long needles. Another factor that could be play a role in this context is aspirin hydrolysis. If exposed to moisture aspirin hydrolyses to acetic acid and salicylic acid which could also lead to tablet softening.

2.5. Near-infrared measurements

The EVK Helios NIR G2-320 Class hyperspectral imaging system was used for analysing the caffeine tablets. This system is working within the spectral range from 0.9 to 1.7µm and acquires complete spectral images line by line for each local pixel in parallel. The detector has a spatial resolution of 320 pixels with a size of 30 x 30µm. An indium gallium arsenide sensor is used for detection. In the investigation of aspirin tablets the EVK Class Helios SWIR Core was applied. This spectrometer has a spectral range from 1.3 to 2.3µm and is also working in line-scanning mode. The system acquires pixels with a size of 30 x 30µm with a spatial resolution of 256 pixels. Unlike the EVK Helios NIR G2-320 Class system it uses a mercury cadmium telluride sensor. [c]

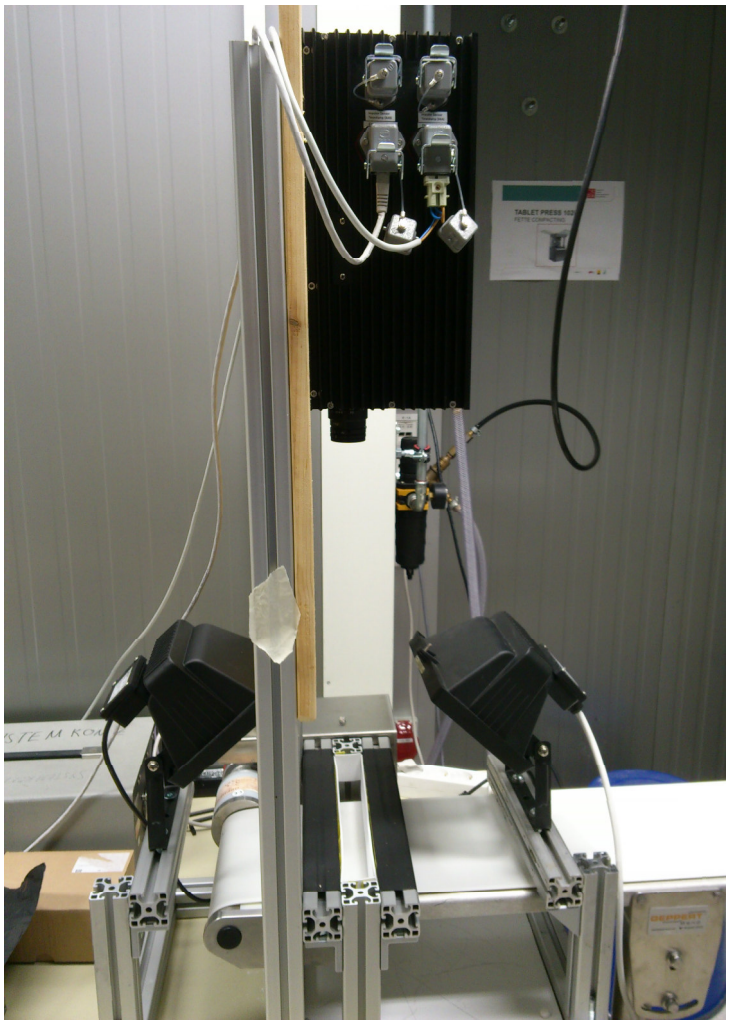

Figure 12: Equipment configuration using the EVK Helios NIR G2-320 Class hyperspectral imaging system.

[c] Cf. EVK product information

Figure 12 shows the equipment configuration using the EVK Helios NIR G2-320 Class hyperspectral imaging system. The spectrometers were fixed on a wooden panel. At a definite distance two light sources were mounted to guarantee constant illumination. In order to achieve a proper diffused lighting Teflon panels were attached to aluminium profiles. The residual aluminium surfaces were covered to prevent additional unwanted reflections, as can be seen in figure 13. The conveyor belt was responsible for moving the tablets through the spectrometers field of view at constant speed.

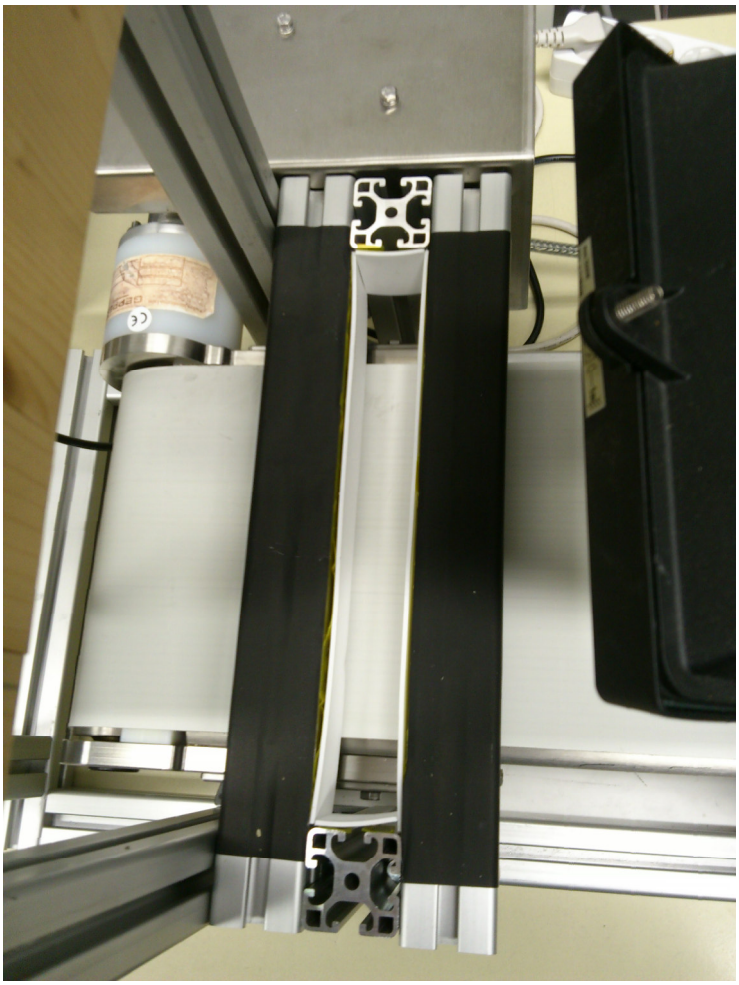

Figure 13: Aluminum construction and conveyor belt.

To prevent changing parameters over the measurement period the light sources as well as spectrometer and conveyor belt were switched on before starting the sample analyses to pre-heat the light sources and thermally equilibrate the spectrometer.

Before starting the tablet investigation black and white balance were measured. Since detectors hold a wavelength dependent dark current, this procedure is very important. The term dark current refers to the detector response given when there is no signal recorded. The dark response is measured by blocking the lens in order to generate a ~0% reflectance signal. The white response is generally obtained by acquiring spectra from a high reflectance standard (~100% reflectance). For the tests Teflon was used as standard for the white balance. Reflectance can then be calculated applying the following equation

$$R = \frac{I - D}{W - D}$$

where R is the relative reflectance image, I the raw reflectance image, D the dark reference and accordingly W the white reference.

Absorbance is defined as the negative decadic logarithm of the above described reflectance.

2.6. UV/Vis measurements

The UV/Vis measurements were conducted using a Perkin Elmer Lambda 950 spectrometer in a wavelength range from 200 to 400nm. The cuvettes used were high precision quarz suprasil cells with a light path of 10mm purchased from Hellma Analytics.

Before determining the API concentration using UV/Vis spectroscopy the tablet's crushing strength was identified. Afterwards the resulting tablet pieces were at first weighted and then transferred in 1000ml volumetric flasks where they were shaken in a small volume of medium for a while until they were almost entirely dissolved. Then the flasks were filled up and capped. The solutions were stirred until the entire tablet was dissolved in the medium. All the samples were filtered through 0.22µm MCE filters purchased from ETI in order to minimize the scattering effects that could be caused by excipients.

For both APIs calibration models were established in the dissolution media. Calibrations in hydrochloric acid at a pH-value of 3.1 were used for the determination of the concentration in the dissolution tests as well and therefore span over a broader concentration range. For the caffeine tablets an additional calibration in water was performed since the tablets pieces were dissolved in distilled water while all of the Aspirin tablets were suspended in acidic solution.

2.6.1. Aspirin tablets

For the aspirin calibration a 100mg/l stock solution was prepared by dissolving 25mg acetyl salicylic acid in 250ml hydrochloric acid solution with a pH value of 3.1. This solution was then gradually diluted with acidic solution. The calibration curve's linear equation was used for the determination of the aspirin concentration present in the tablets as well as for the interpretation of dissolution data therefore it spans over a broad concentration range.

The tablet's theoretical API concentration should be located between 43.56mg and 68.91mg.

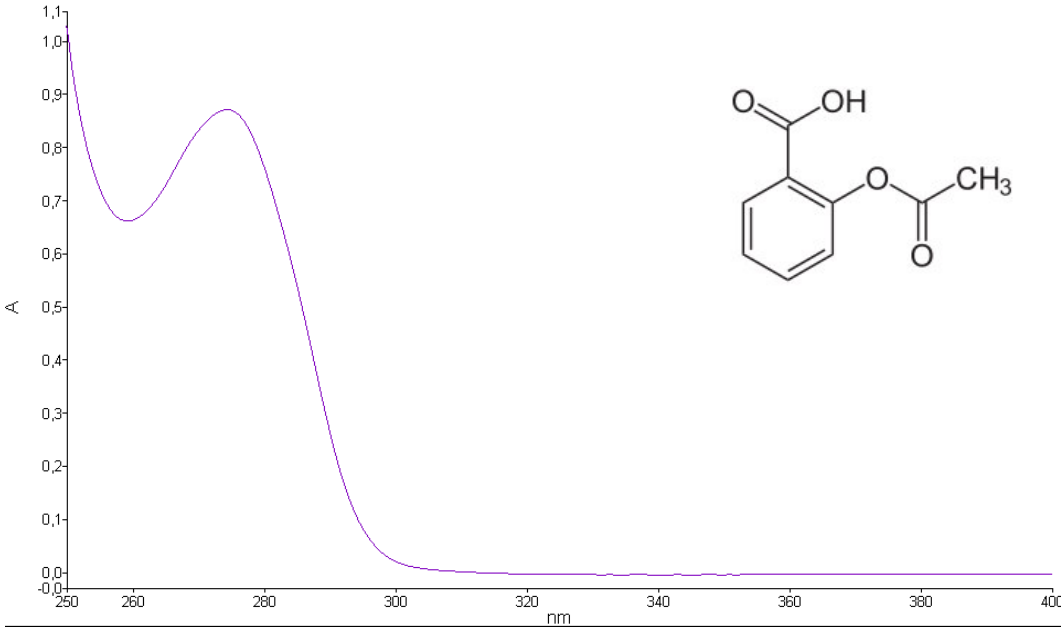

Figure 14: UV/Vis spectrum and structural formula of acetyl salicylic acid.

Figure 14 depicts the UV/Vis spectrum of acetyl salicylic acid in the spectral range from 250nm to 400nm as well as its structural formula. For the calibration and the following measurements the absorption maxima between 274nm and 276nm were used.

2.6.2. Caffeine tablets

The caffeine calibration in water was used to calculate the tablets caffeine concentration. For preparing a stock solution 6.96mg pure caffeine were dissolved in 200ml distilled water. This solution was then gradually diluted with distilled water. With the resulting linear equation the caffeine concentration for the measured absorption values could be determined. For this calibration a concentration interval between 17mg/l and 35mg/l was chosen as the theoretical caffeine concentration per tablet should be located between 21.78mg and 33.86mg.

For the dissolution measurement data another calibration was established in acidic solution. A stock solution was prepared by dissolving 10.06mg caffeine in 250ml hydrochloric acid solution at a pH value of 3.1. Again this stock solution was gradually diluted with acidic solution. The resulting curve spanned over a broader concentration range in order to be able to determine the caffeine concentration in every dissolution step.

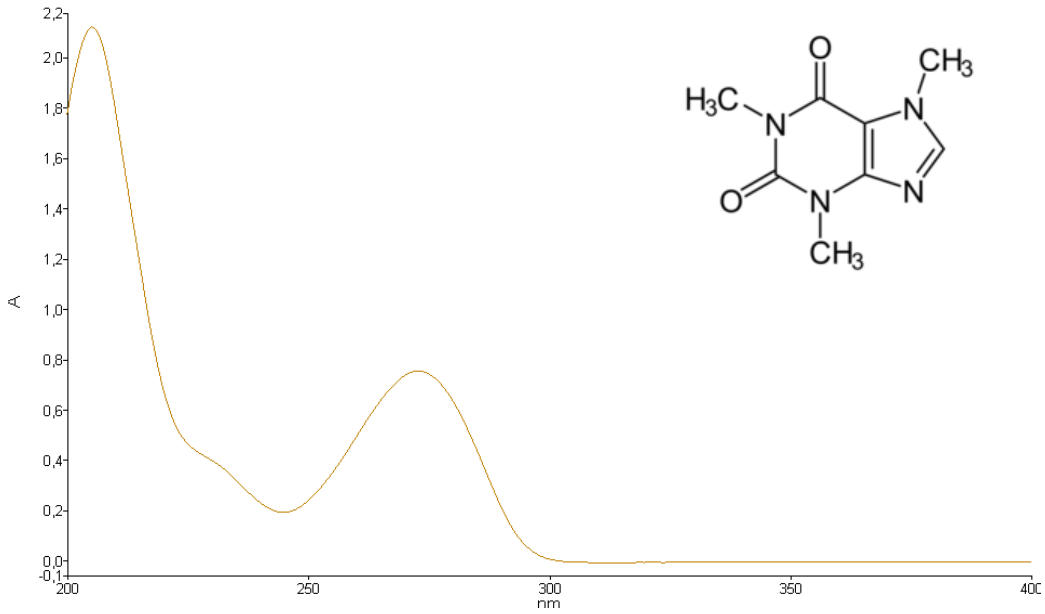

Figure 15: UV/Vis spectrum and chemical formula of caffeine.

Figure 15 shows the UV/Vis spectrum of caffeine dissolved in acidic solution as well as the structural formula of caffeine. The absorption values were determined at the maximum between 272nm and 274nm.

2.7. Dissolution testing

1l of dissolution medium was filled into the vessels and heated up to 37°C according to the specifications in the US Pharmacopeia. During the heating the medium was stirred at 100rpm. While the tablet was inserted, the paddle stirrers were stopped to ensure sinking without turbulences und to prevent the paddle from hitting the sample. When the tablet was inserted the test was started immediately at a rate of 100rpm. Samples of 3ml were taken at the chosen time points. They were filtered through 0.22µm filters shortly after the sampling in order to minimize scattering effects that might influence the measurements as well as to remove not dissolved small tablet pieces that could dissolve later and result in false absorption values. All of the samples were taken with syringes midway between the rotation blade and the surface of the dissolution media as described in Pharmacopeia.

The volume used for the measurements was not restored as described in the Pharmacopeia. However the volume change was compensated in the calculations. Nonetheless, after the tablets were completely dissolved no volume compensation was necessary.

It is recommended to degas the media used in the dissolution tests to prevent the formation of bubbles which might change the results. Still the media were not degassed as in the pre-tests no bubble formation could be observed.

Both, aspirin as well as caffeine tablets were analysed with the dissolution tester DT 820 Series from ERWEKA. All the samples were at first investigated using EVK NIR spectrometers, weight and then inserted in the dissolution tester. The solutions were measured with the Perkin Elmer Lambda 950 spectrometer (s. UV/Vis measurements).

2.7.1. Aspirin tablets

For the dissolution tests two tablets of each compression force with an aspirin concentration of 10wt.% were used. The sampling points chosen after performing a pre-test were 1min, 3min, 5min, 7min, 10min, 15min, 20min, 25min, 30min and 45min.

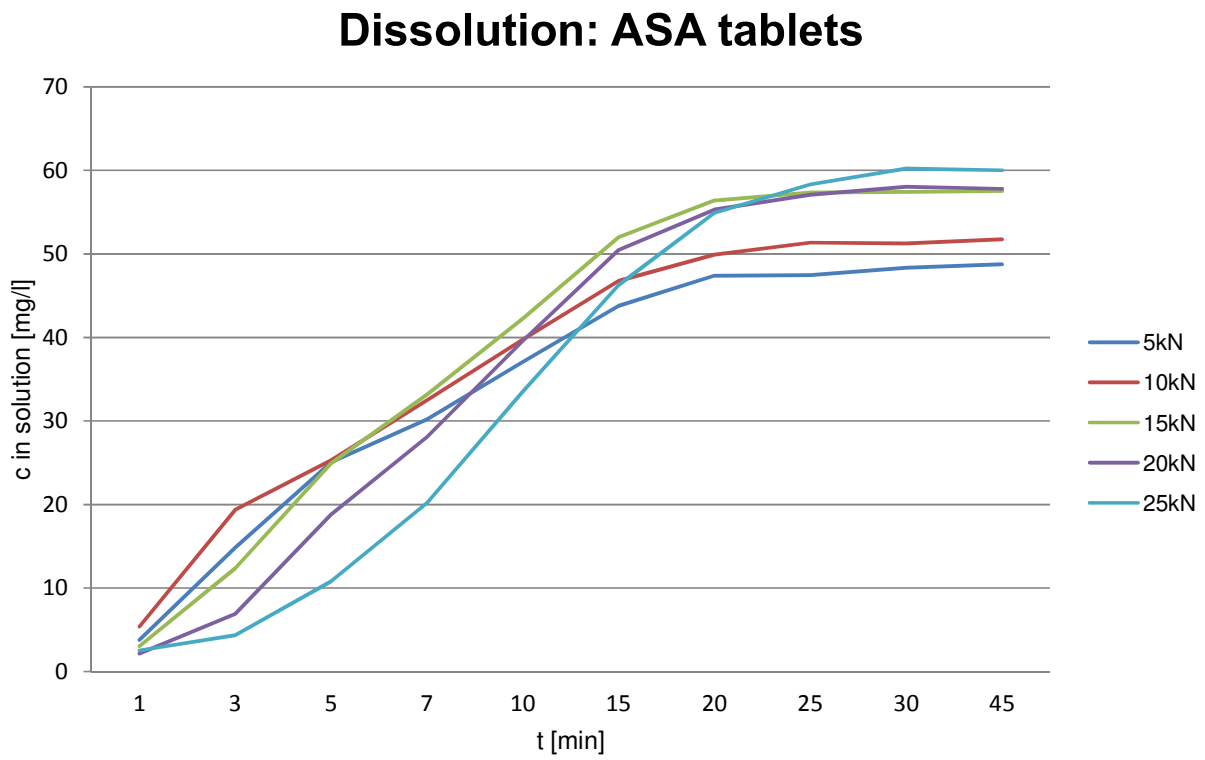

Figure 16: Dissolution profile of aspirin tablets.

The dissolution profile for the first five aspirin tablets is pictured in figure 16. Tablets produced at lower compression force were totally dissolved after about 20 to 25 minutes while the ones manufactured with higher compression forces took approximately 30 minutes. It can also bee seen that the detected API concentration in solution varies strongly. This might indicate that the powders used for the production of these tablets were not mixed properly or segregated during feeding in the tablet press. Still figure 16 significantly shows that tablets produced at low compaction forces dissolve faster than tablets with high compaction forces.

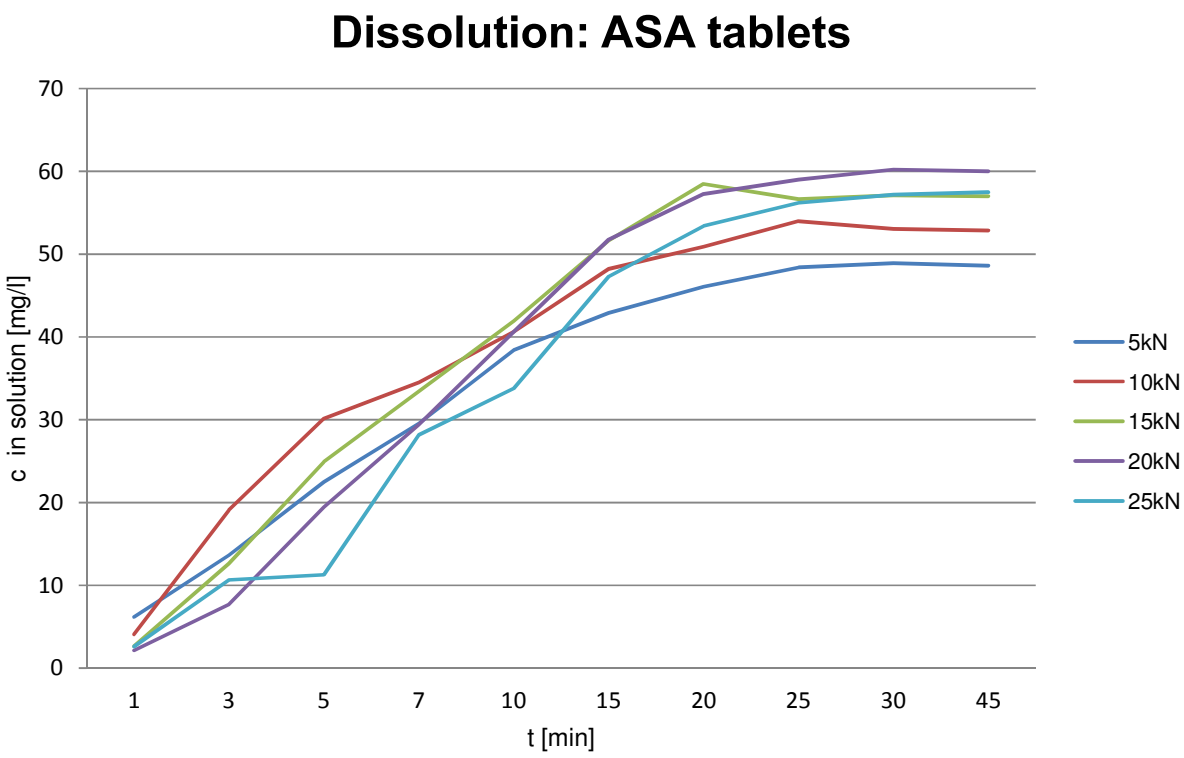

Figure 17: Dissolution profile aspirin tablets 10wt.%.

In figure 17 the dissolution profile of the following 5 aspirin tablets is shown. Again it can be observed that tablets with a low compression force are dissolved faster and have a lower API concentration.

2.7.2. Caffeine tablets

Caffeine tablets showed very similar dissolution properties besides the fact that they are even faster dissolving than the aspirin tablets. Therefore, the same time points were chosen for sampling.

In each case six tablets with the highest (6wt.%) and lowest (4wt.%) API concentration were tested. Half of them compressed with the highest (30kN) and half with the lowest (5kN) compaction force.

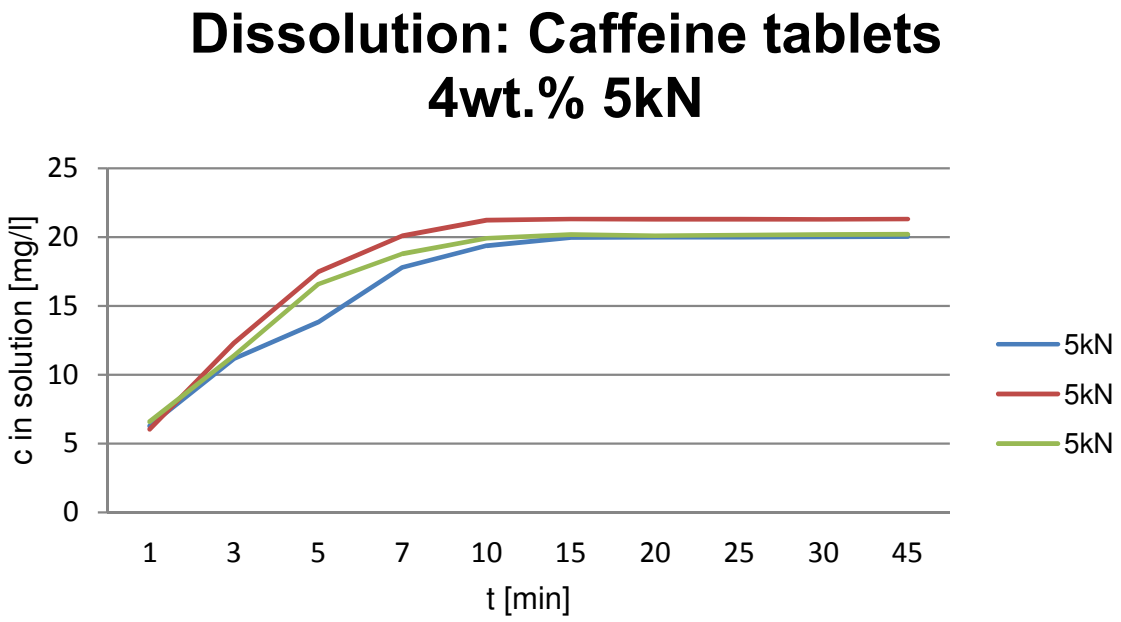

Figure 18: Dissolution profile of 4wt.% caffeine tablets produced at 5kN.

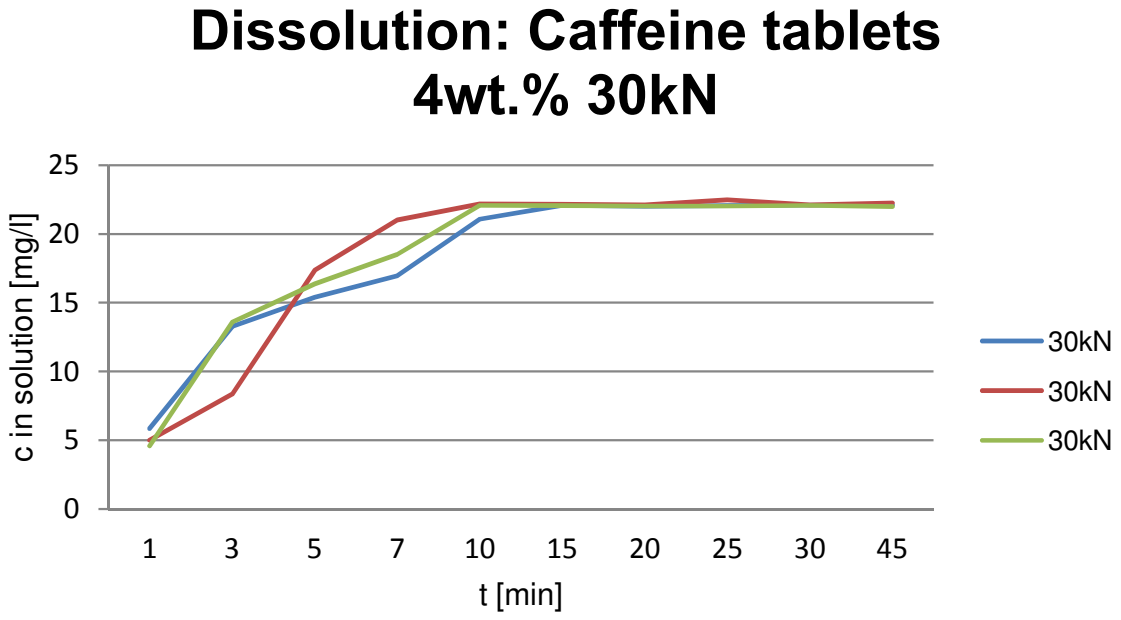

Figure 19: Dissolution profile of 4wt.% caffeine tablets produced at 30kN.

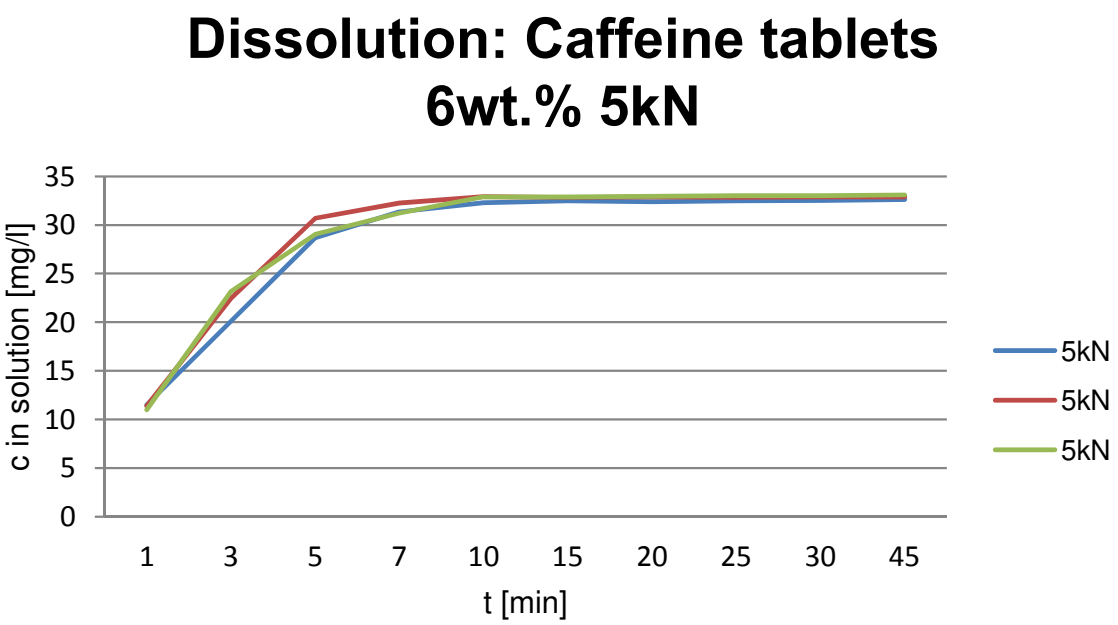

Figure 20: Dissolution profile of 6wt.% caffeine tablets produced at 5kN.

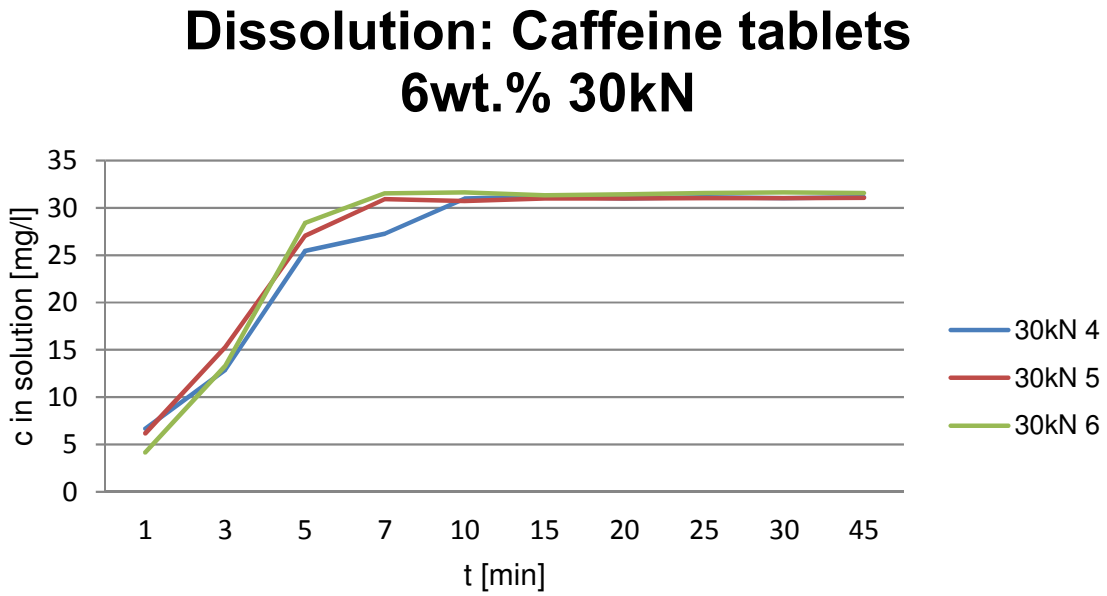

Figure 21: Dissolution profile of 6wt.% caffeine tablets produced at 30kN.

All the samples were completely dissolved after 15 minutes. The caffeine powder mixtures seem to be blneded properly since the end point concentrations are located within the same ranges. For the 4wt.% samples the end points spanned between 20.0mg/l and 22.3mg/l in solution. The 6wt.% tablets reached concentrations between 31.1mg/l and 33.1mg/l.

Examining the caffeine concentration at the first time points a striking difference between the 4wt.% and the 6wt.% samples can be observed. While the 4wt.% samples show nearly the same curve progression independent from compaction force, the 6wt.% tablets exhibit a great difference in their dissolution profiles. These samples also show more constant curve progression.

Generally tablets tend to dissolve more slowly with increasing compaction force. This trend can be seen for aspirin as well as for caffeine tablets. Still caffeine samples do not show strong differences as they disintegrate a lot faster then the aspirin tablets.

Results and Discussion

3.1. Aspirin tablets

A total of 235 aspirin tablets were analysed in order to set up a chemometric model for the determination of compaction force and API content applying NIR spectroscopy.

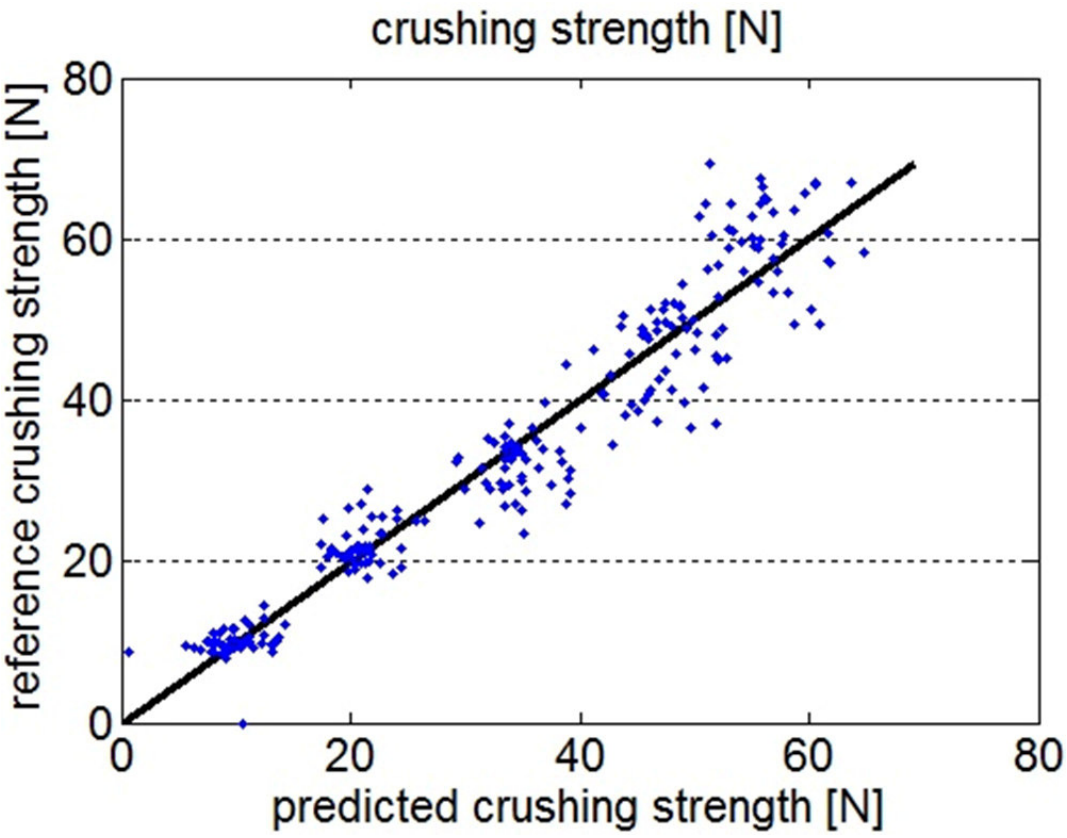

Figure 22: ASA tablet's reference and predicted crushing strength values.

Figure 22 presents the results of the reference crushing strength values plotted against the predicted values. The data points at low crushing strength are closely spaced while at higher crushing strength a broader distribution can be observed.

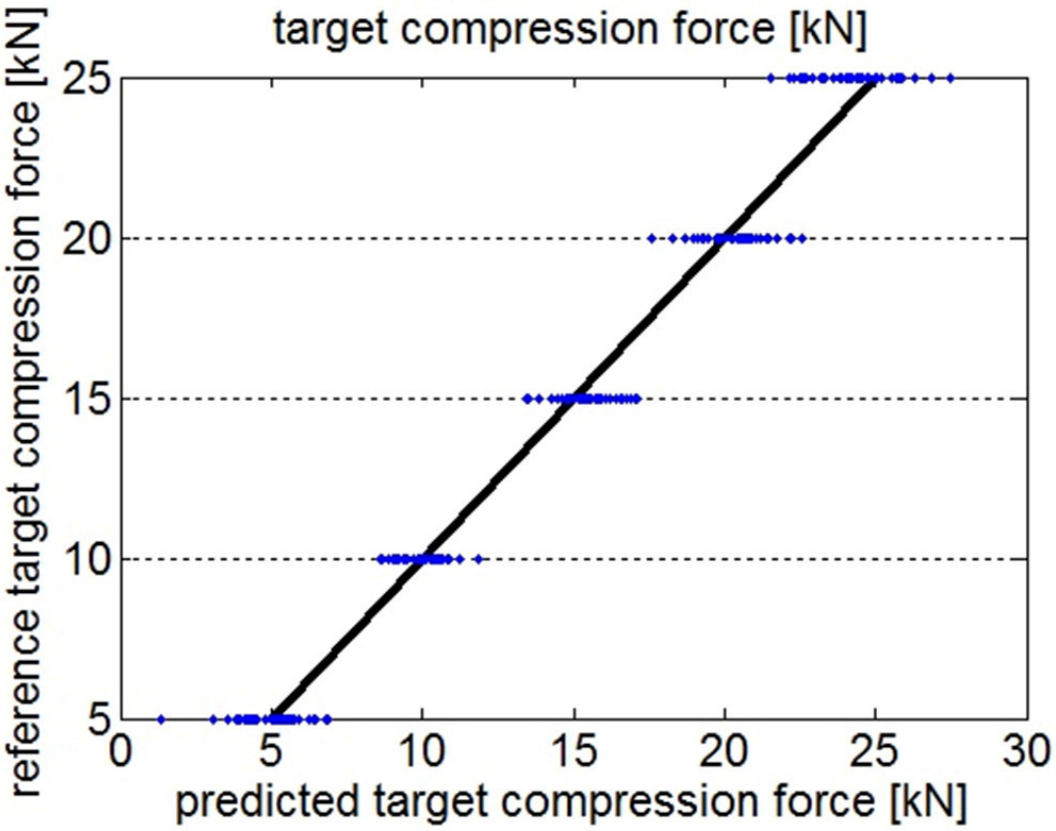

Figure 23: ASA tablet's reference target and predicted target compression force.

In figure 23 reference target compression force and predicted target compression force are depicted. Again it can be observed that the distribution at higher compression force values broadens.

When discussing tablet compression force and crushing strength it has to be kept in mind that during the fabrication process compression forces varied due to variations in the fill level of the die. This explains the apparent data point distribution in figure 22 and 23. Still as can be observed in figure 23 the data points are statistically spread around the target values and achieve a good result.

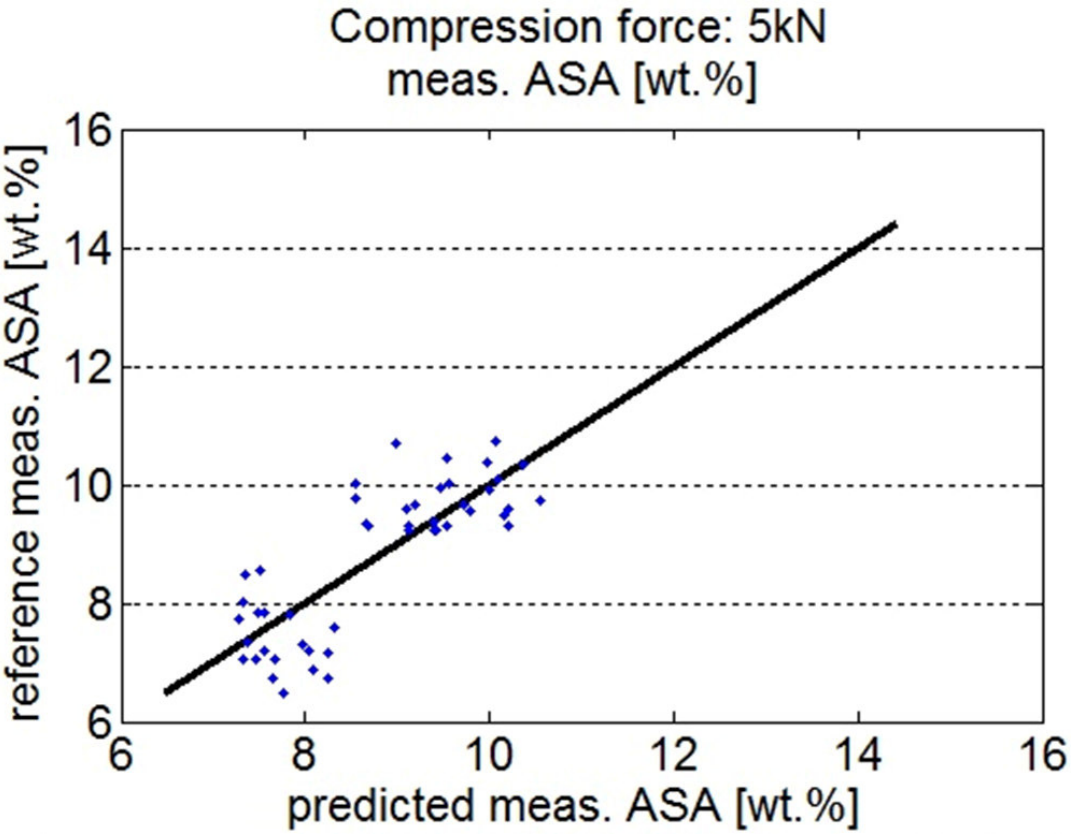

Figure 24: Reference and predicted ASA concentration at a compaction force of 5kN

In figure 24 the reference and predicted API content at a compression force of 5kN is depicted. Although tablets with a target aspirin concentration spanning from 8wt.% to 12wt.% were investigated an API content of 12wt.% could not be detected. Generally data points indicate concentrations below the target aspirin concentration. The UV/Vis reference measurement findings are presented in figure 25 showing the deviation from the calculated target API concentration for every aspirin tablet produced at a compression force of 5kN. Nearly all data points are located distinctly below the target concentration and only a few have a higher concentration than the value expected. Moreover compared to the other reference data the values seam rather randomly distributed.

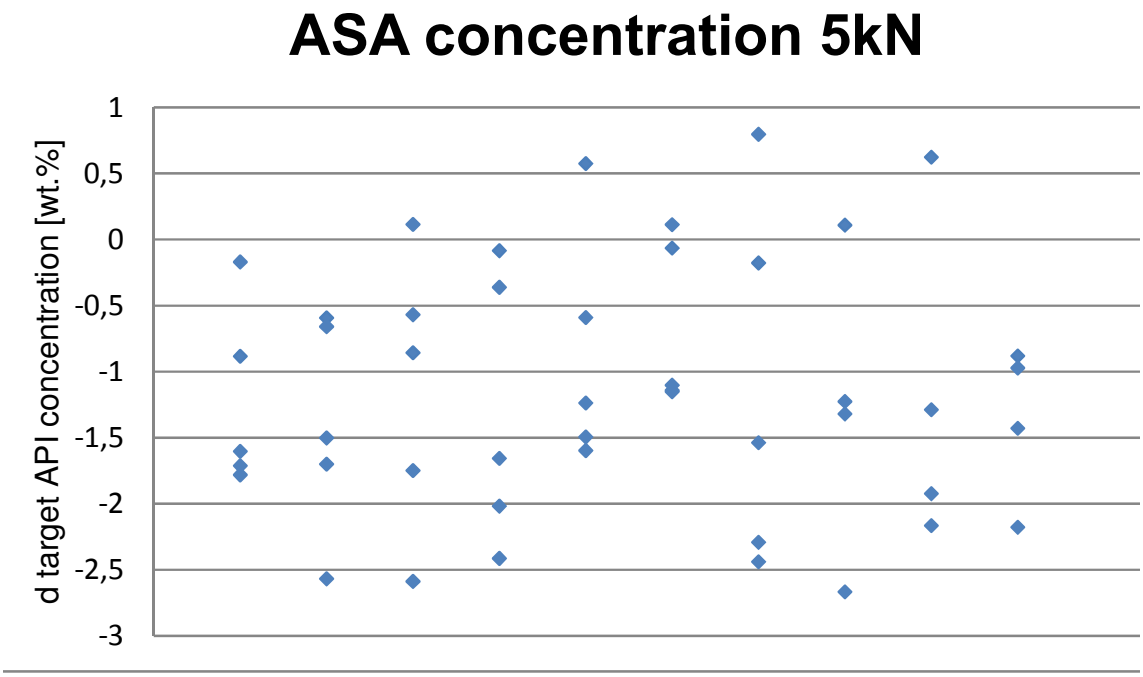

Figure 25: Reference ASA concentration at 5kN.

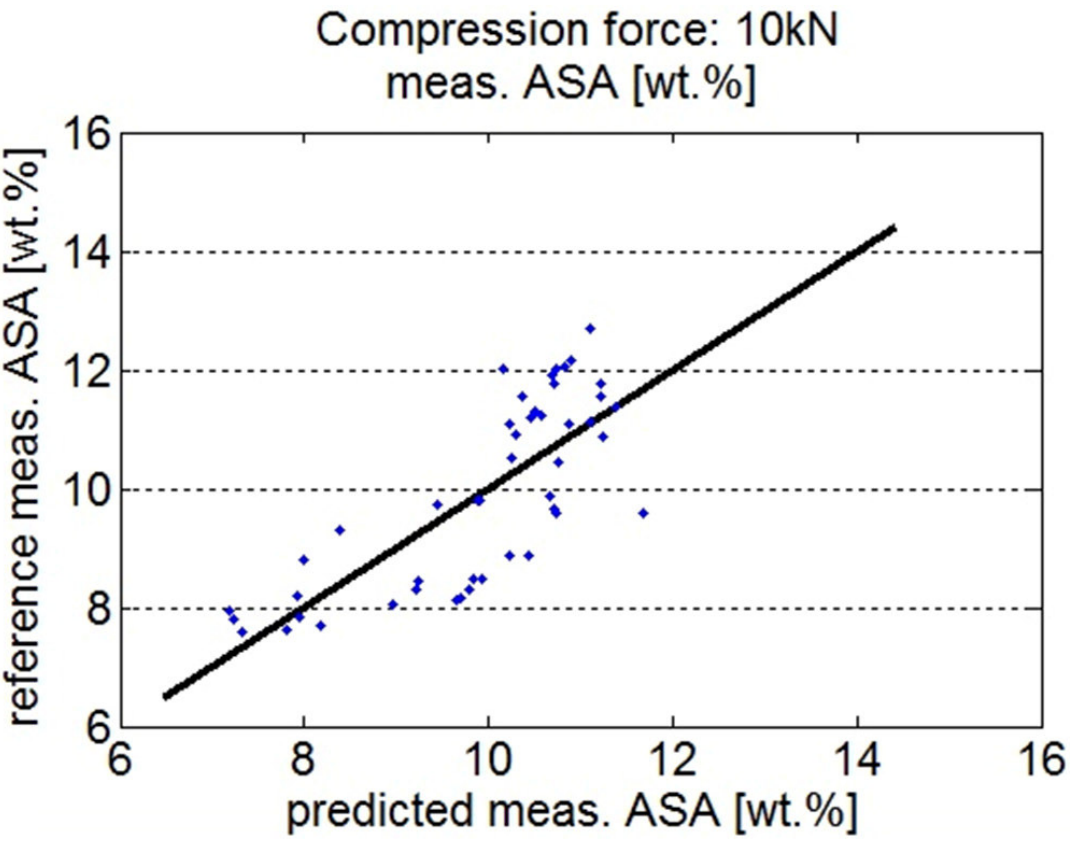

Figure 26: Reference and predicted ASA concentration at a compaction force of 10kN.

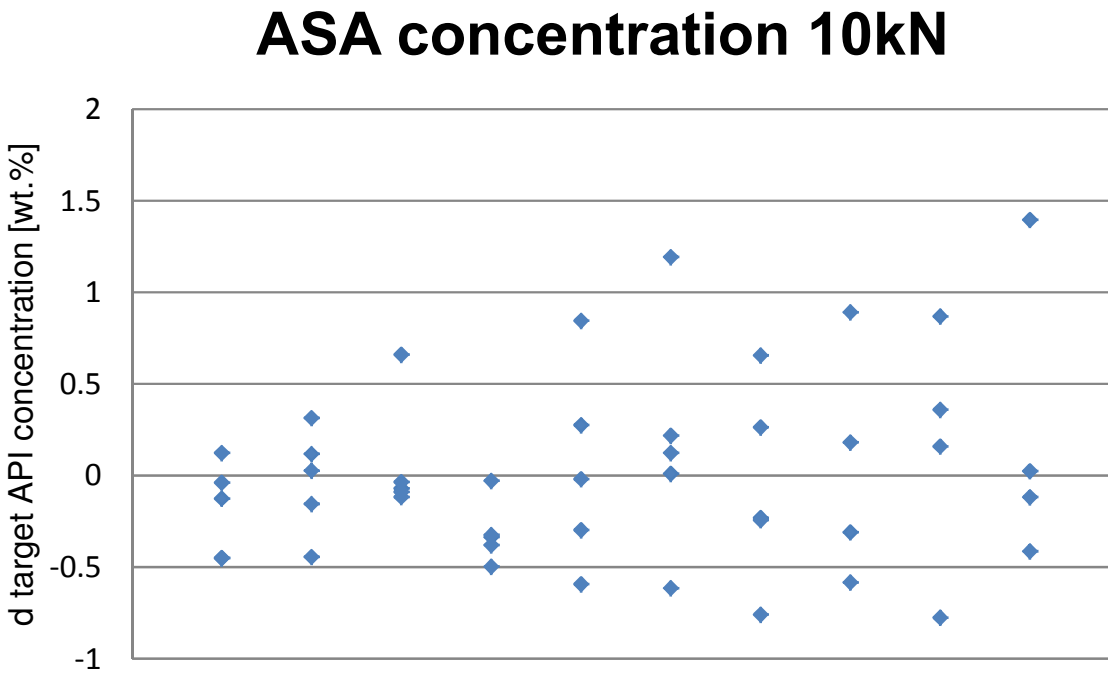

Figure 27: Reference ASA concentration at 10kN.

The tablets produced at 10kN show a similar behaviour. Many of these samples express lower aspirin concentrations than expected but they still have higher API concentrations than the tablets produced at 5kN.

Comparing figure 27 with the reference data generated for the other compression forces the tablets produced at 10kN seam to have concentrations closest to the target API content. Here the majority of the data points can be found within a deviation of 0.5wt.% from the target value. Looking at the higher compression forces like 15kN and 20kN concentrations are constantly increasing as can be seen in figures 28 to 31.

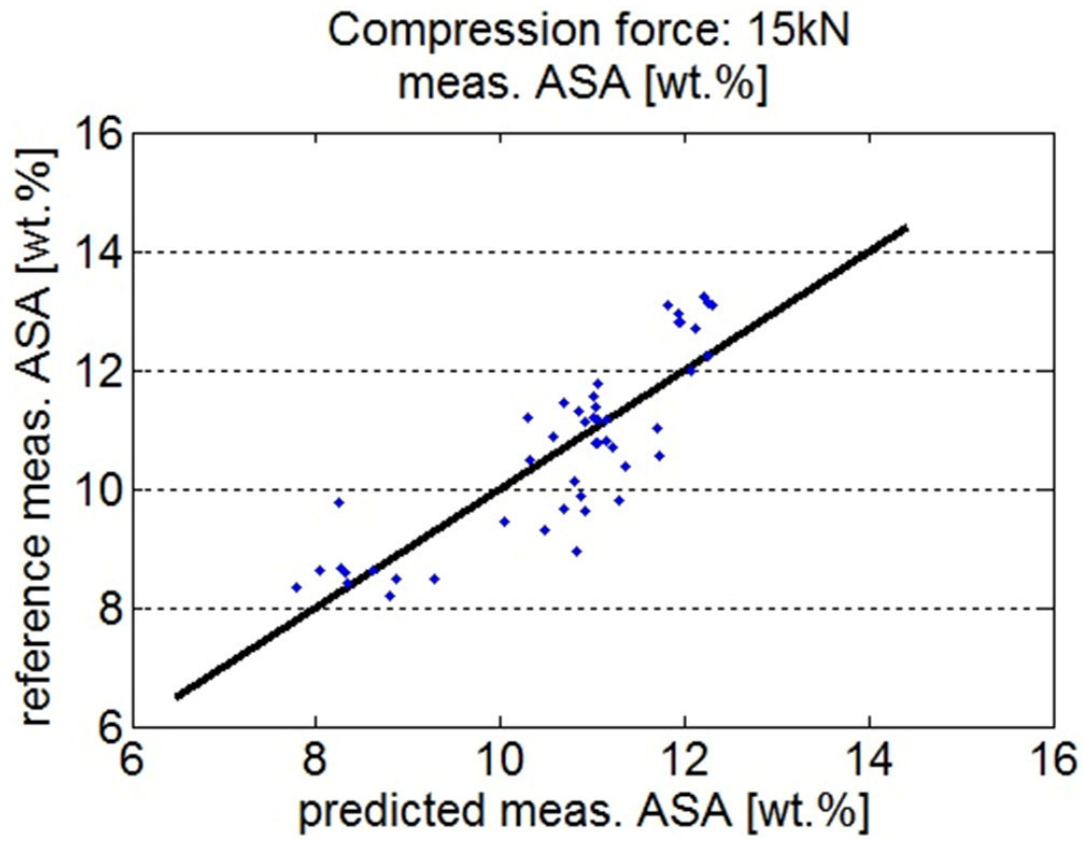

Figure 28: Reference and predicted ASA concentration at a compaction force of 15kN.

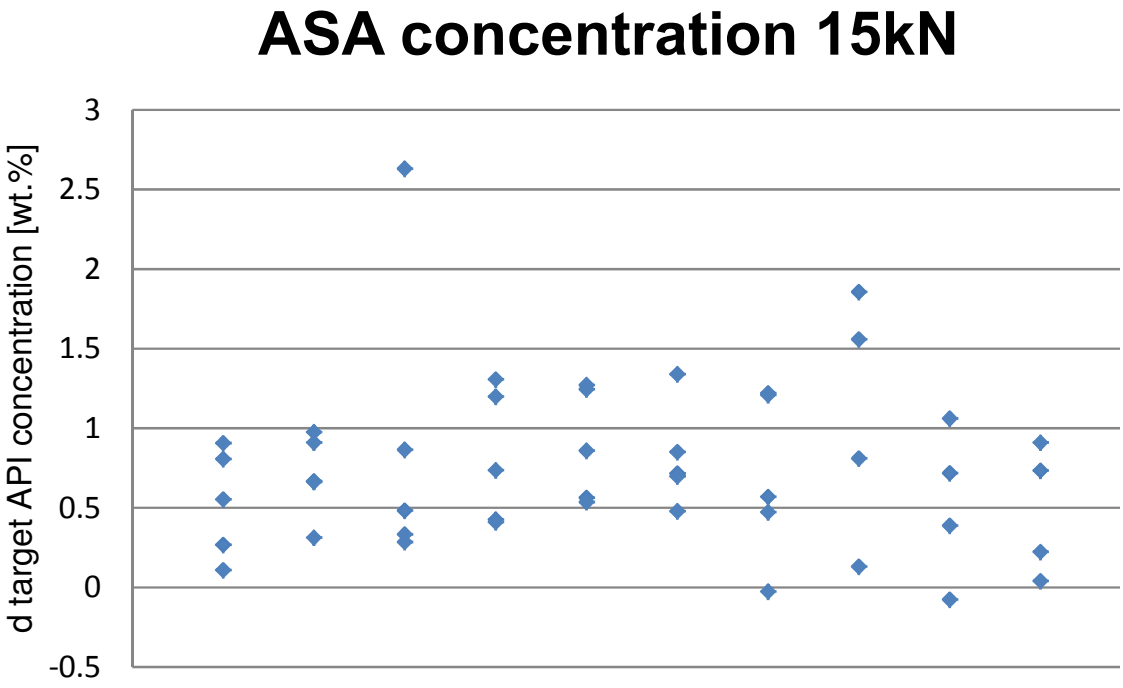

Figure 29: Reference ASA concentration at 15kN.

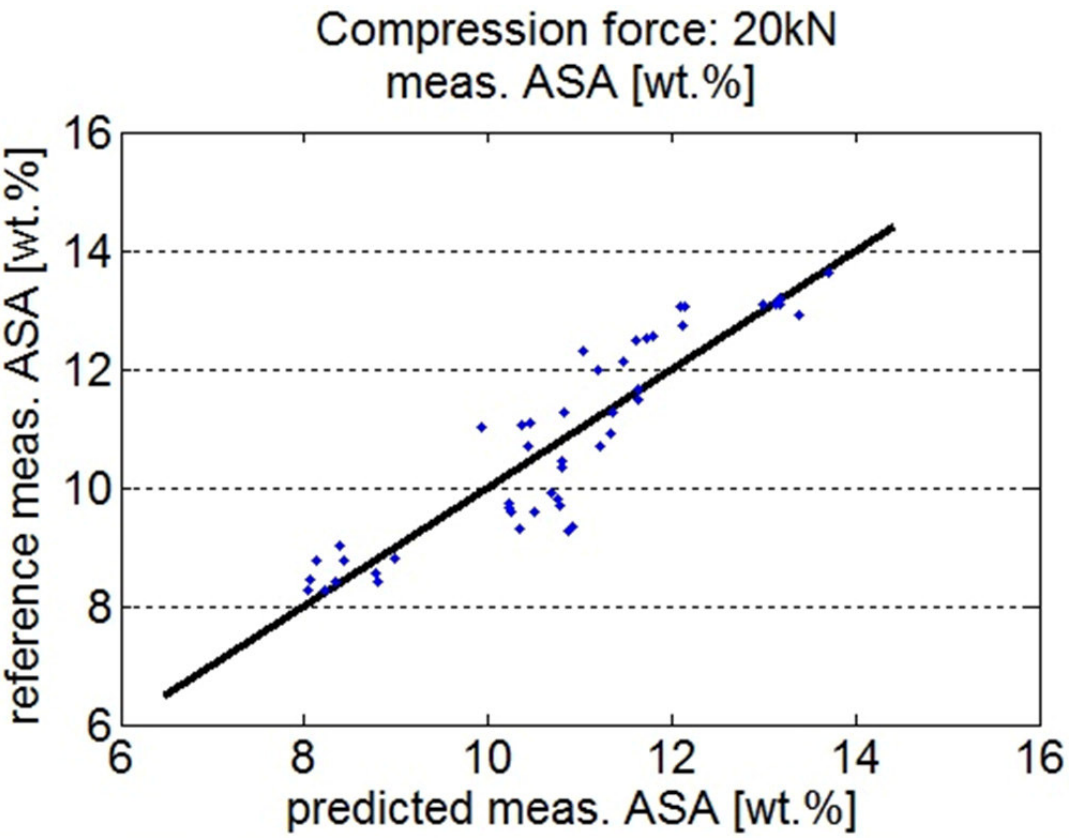

Figure 30: Reference and predicted ASA concentration at a compaction force of 20kN.

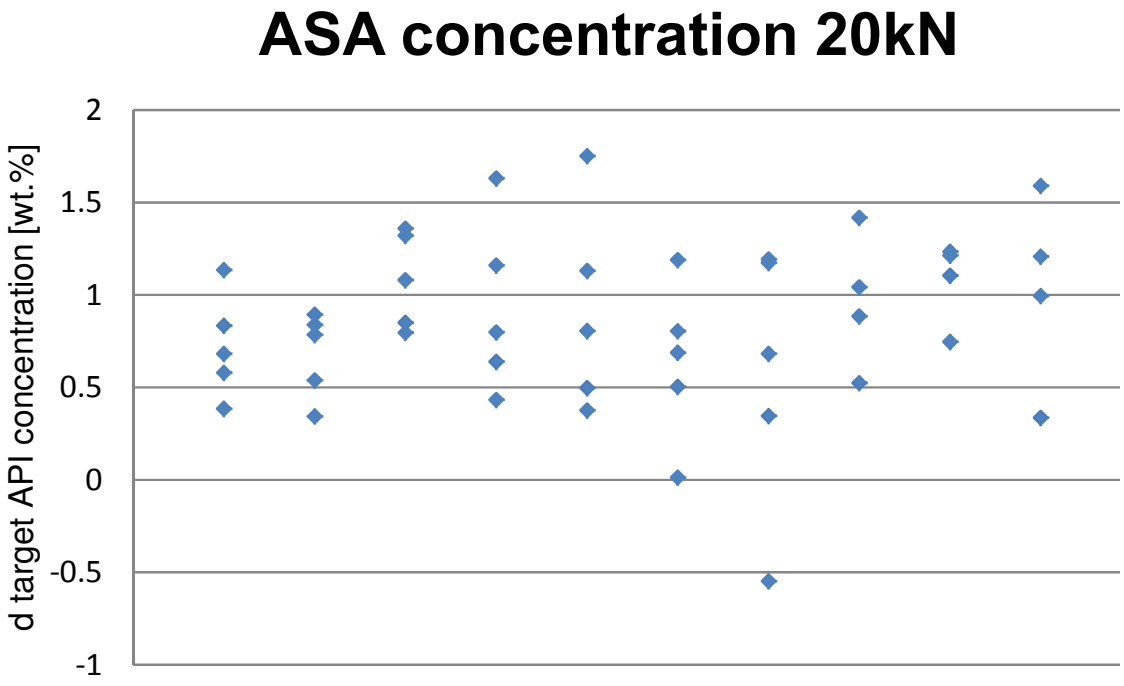

Figure 31: Reference ASA concentration at 20kN.

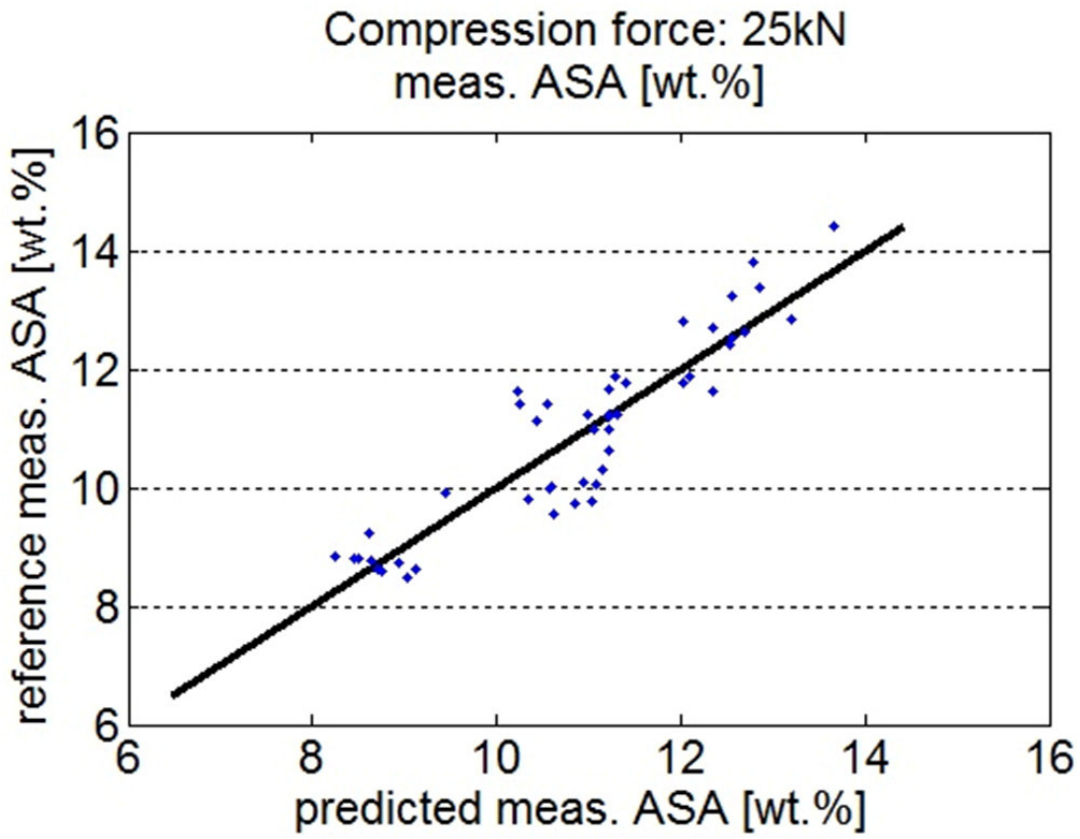

Figure 32: Reference and predicted ASA concentration at a compaction force of 25kN.

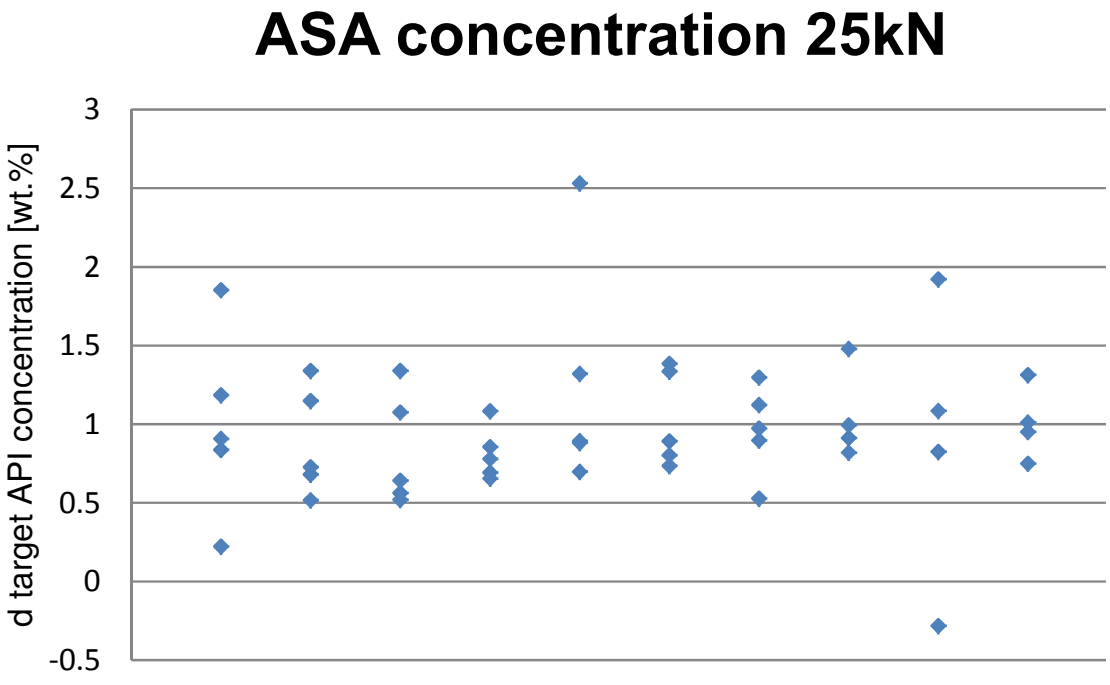

Figure 33: Reference ASA concentration at 25kN.

This trend also continues for the highest compression force where, as expected, the highest API concentrations can be detected. At 8wt.% no data points can be observed while many exceed the theoretical maximum concentration of 12wt.%. The reference measurement results for tablets produced at 25kN show that the majority of data points can be found within 0.5wt.% and 1.5wt.% deviation form the target aspirin concentration values. Therefore, for most of the tablets an API concentration within 8.5wt.% and 13.5wt.% can be expected.

Analyzing the data generated in the measurements, it can be observed that low compression forces show only small acetyl salicylic acid concentrations while at high compression forces greater concentrations can be determined. Tablets produced at the lowest compaction force have an API concentration far below the target content. On the contrary tablets produced at greater compression forces exhibit aspirin concentrations much higher than the expected values. This trend indicates segregation processes in the feeder since for all powder mixtures tablets were produced starting from the lowest compaction force further increasing compression until the highest target compaction force was reached. The first tablets produced have a minor API concentration while the last tablets exceed the target values distinctly.

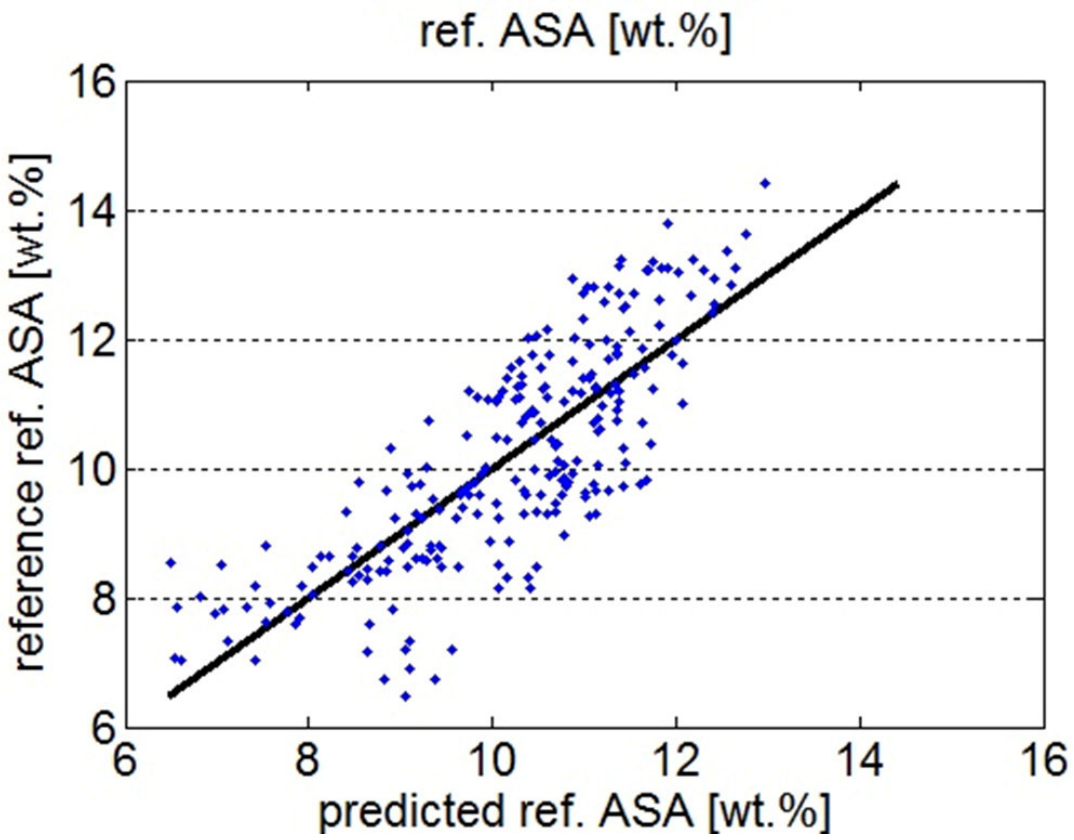

Figure 34: Reference and predicted reference ASA concentration.

In figure 34 the reference and predicted reference aspirin content is shown. It can be observed that many data points can be found in a concentration range distinctly lower than 8wt.% and higher than 12wt.%.

On the whole it shows a very broad data point distribution with many outliers especially in the regions of low API content. For the higher concentrations it can be noticed that the measured reference aspirin concentration often exceeds the predicted reference values.

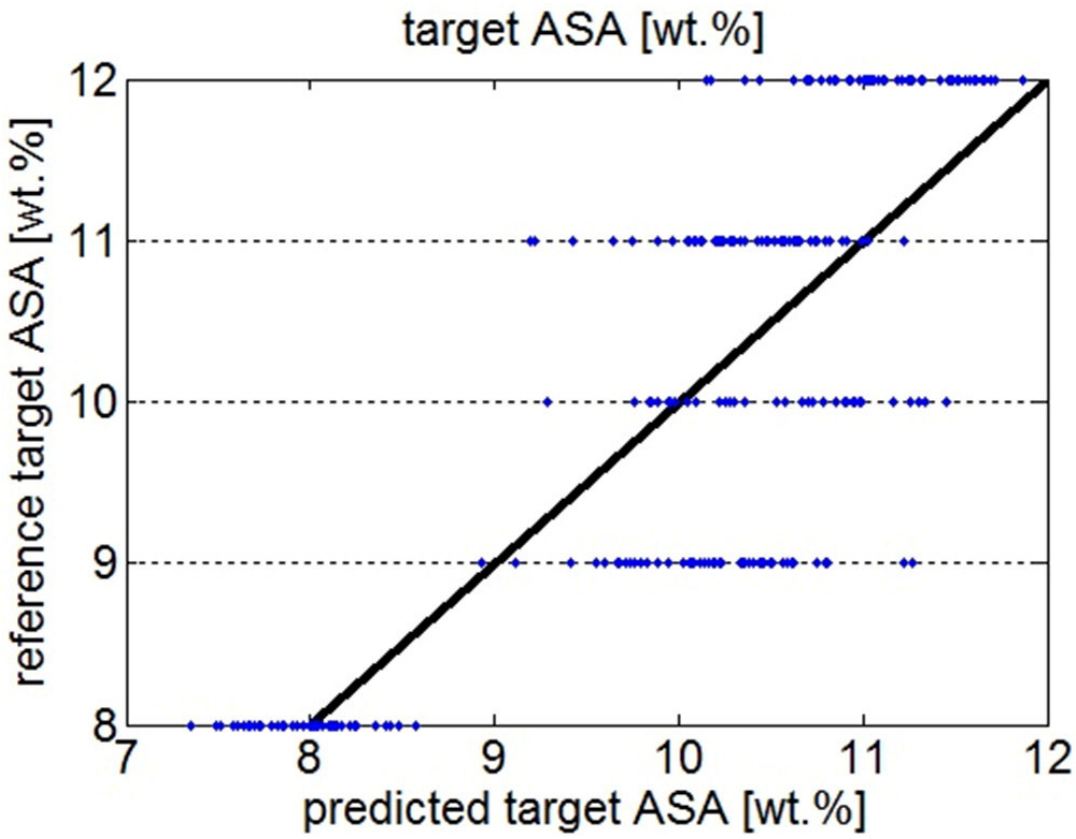

Figure 35: Reference target and predicted target ASA concentration.

Figure 35 shows the predicted target acetyl salicylic acid concentration plotted against the reference target concentration. Strikingly only the data points for the predicted target aspirin concentration at a reference content of 8wt.% are statistically distributed around the expected percentage. The tablets with a reference target concentration of 9wt.%, 10wt.% and 11wt.% have predicted target concentrations spanning roughly within the same range. Causing predictions too high for 9wt.% and too low for 11wt.%. Additionally, these three concentrations show a very broad data point distribution. Tablets with an API concentration of 12wt.% show predicted values below the target and a broad distribution as well.

This figure clearly shows the importance of reference analytics for NIR applications. Without proper reference measurements setting up a reliable PLS model is virtually impossible especially with samples showing great deviations from the target values.

3.2. Caffeine tablets

For every caffeine concentration 18 tablets were analysed; three at each compression force.

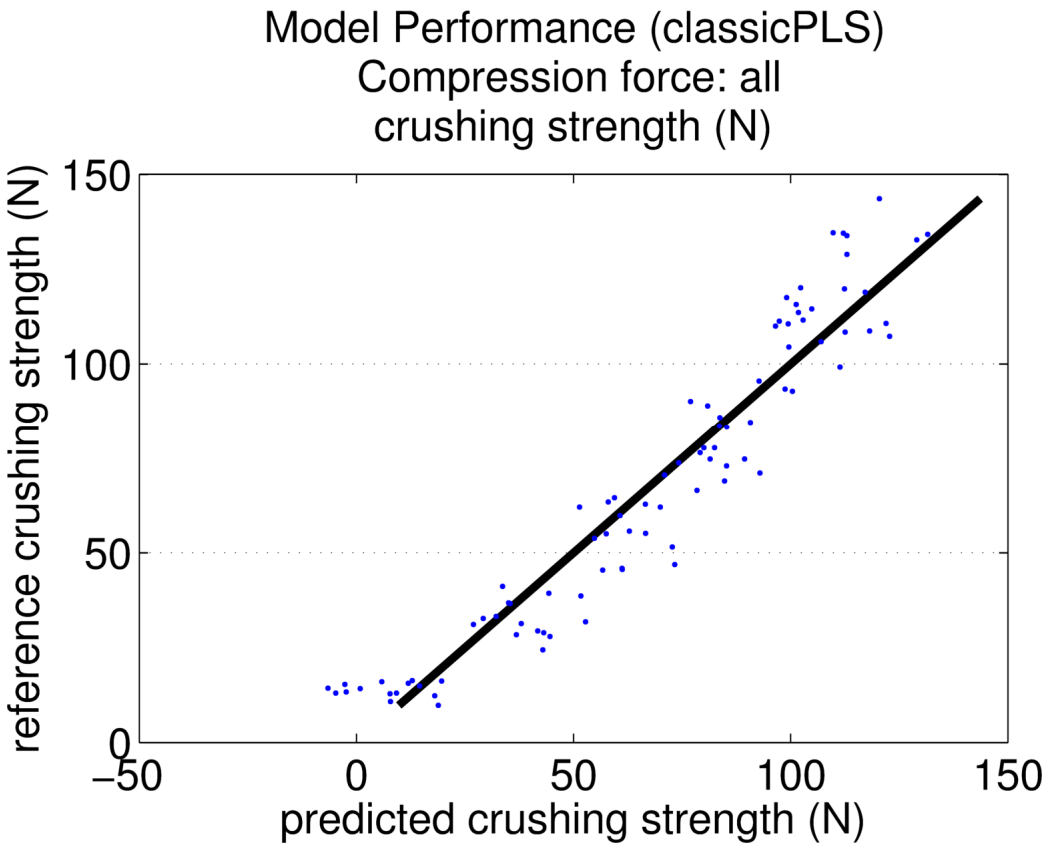

Figure 36: Caffeine tablet's reference and predicted crushing strength values.

Figure 36 depicts the predicted crushing strength and the crushing strength values determined via reference measurements. Within the medium range it appears that the predicted values are higher than the measured reference values. In general the data points are statistically distributed.

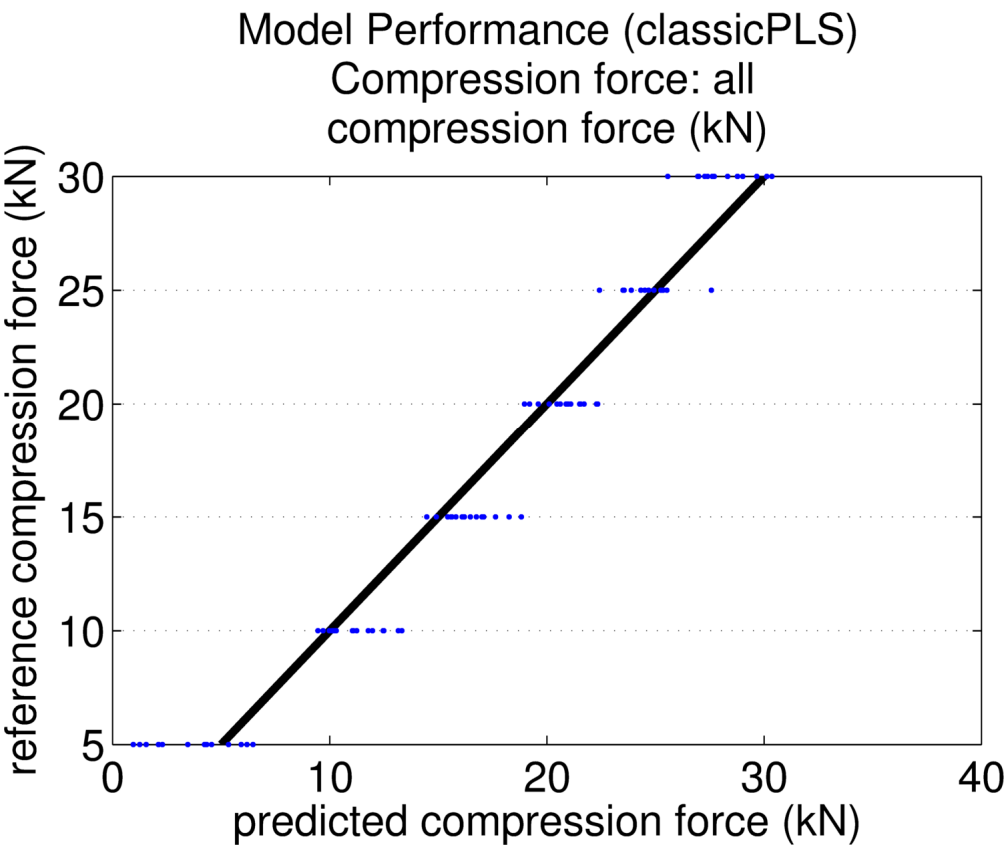

Figure 37: Caffeine tablet's reference and predicted compression force values.

In figure 37 the reference compression force and the predicted compression force are depicted. The data points for the compression forces show statistical distributions around the target values. Since during tablet manufacturing the compression force could not be fixed at a certain value this distribution seems logical.

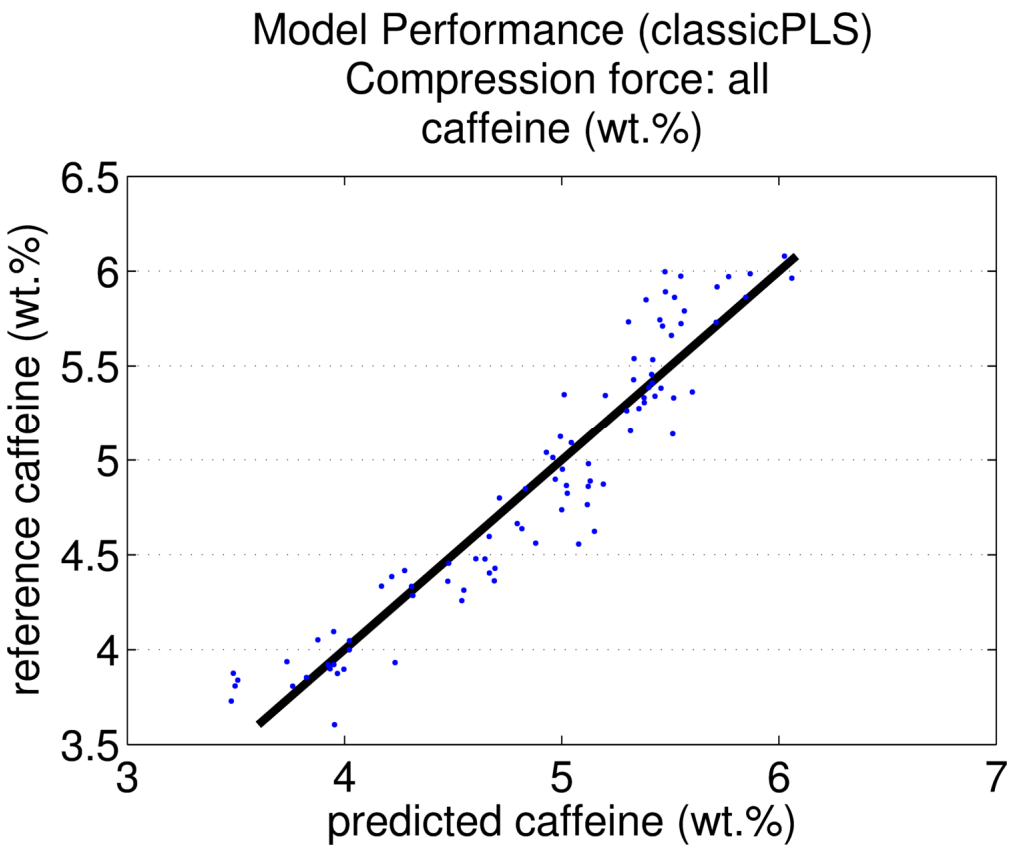

Figure 38: Reference and predicted caffeine content.

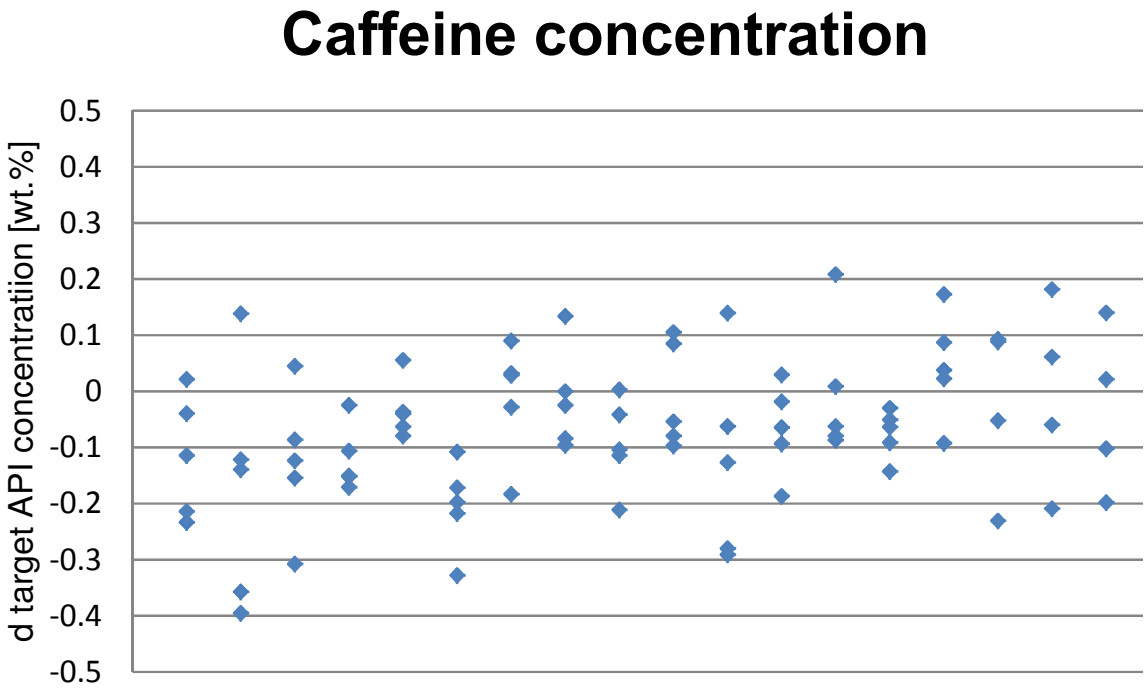

Figure 39: Reference caffeine concentration for all tablets,

The reference and the predicted caffeine content are shown in figure 38. In comparison to the aspirin tablets a narrower distribution can be observed. Additionally, no indication for segregation processes is given. Figure 39 confirms these findings showing the UV/VIS reference measurement's deviation from the calculated target caffeine concentration. The reference data span roughly within -0.4wt.% and 0.25wt.% variance from the target value.

3.3. Conclusion

As described in literature API concentration as well as tablet hardness can be determined using near-infrared spectroscopy. In order to set up a chemometric model, detailed and reproducible reference analytical methods are indispensable as well as the utilization of suitable model substances. With a good sample preparation and enough known parameters a model can be set up with only a few samples.

The employment of reference measurements even for known compositions and substances is of utmost importance because segregation processes during manufacture or insufficient blending can always lead to wrong interpretations, as can be observed for the aspirin tablets. On the contrary the caffeine samples performed well in the determination of API content. Generally well-blend, non-segregating powder mixtures do not require as many points for the creation of a model.

Both APIs obtained good results for the reference and NIR hardness measurements at every compression force. In addition to the determination of tablet hardness other physical properties like the tablet's dissolution behaviour can be predicted. A potential improvement for the compression force or tablet hardness identification would be investigating tablets produced at a known compression force rather than taking samples from a process set at a certain value. Different compaction forces lead to a distribution in hardness and therefore crushing strength as can be observed in the tests.

Appendix

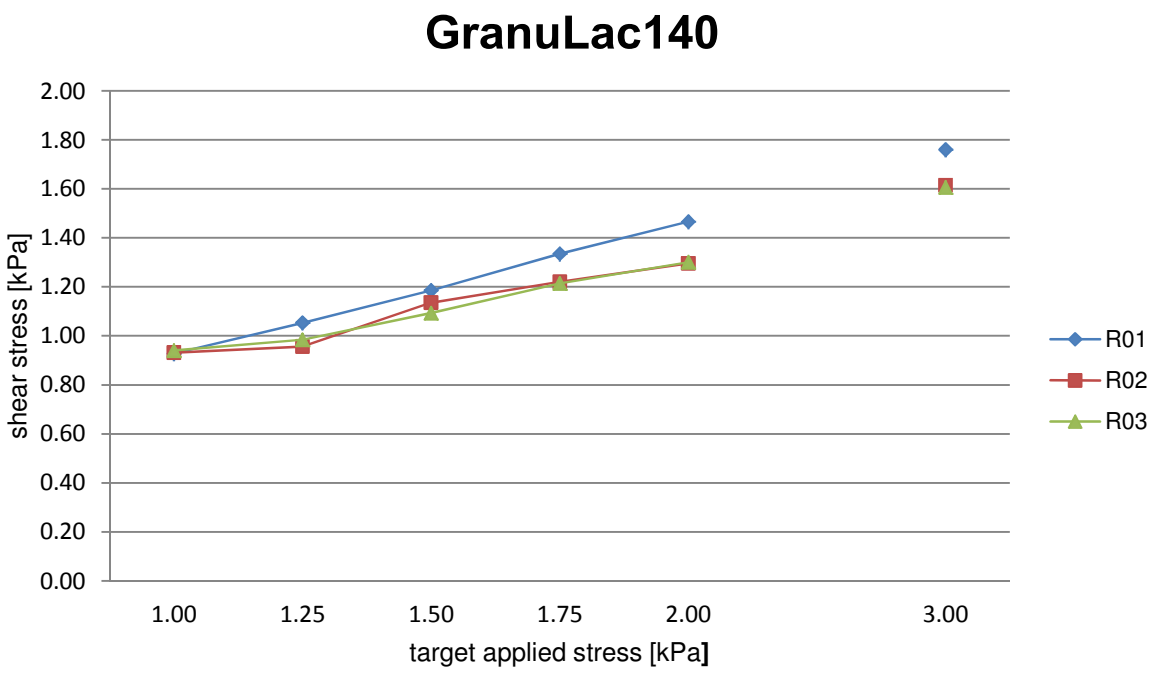

Figure 40: GranuLac140 yield loci.

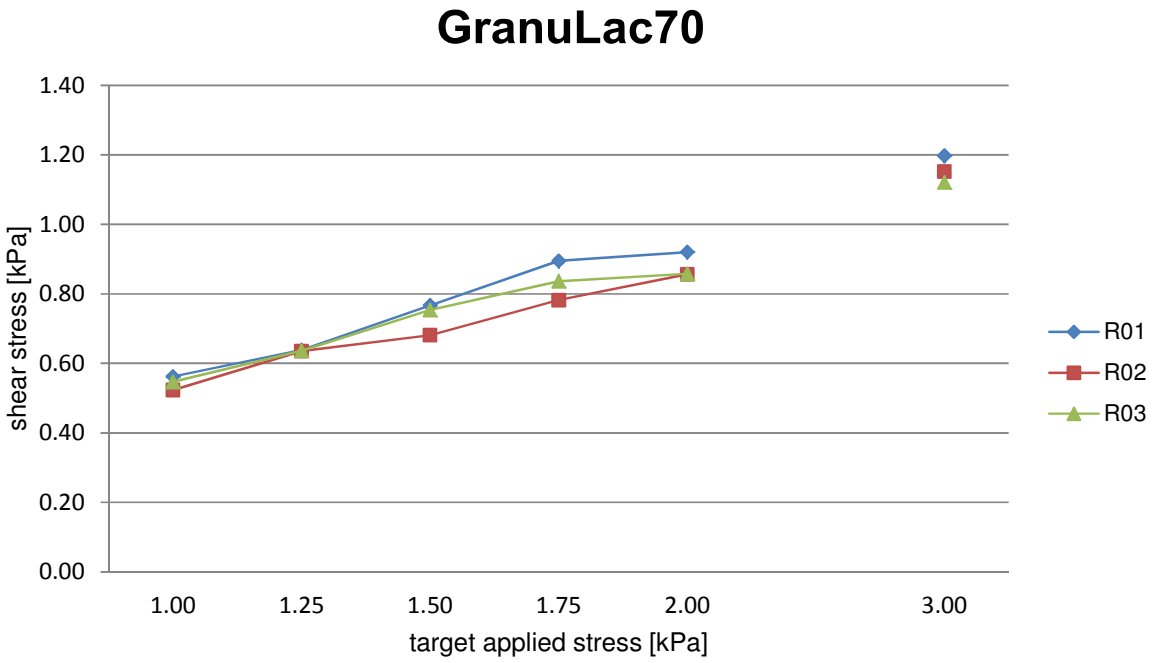

Figure 41: GranuLac70 yield loci.

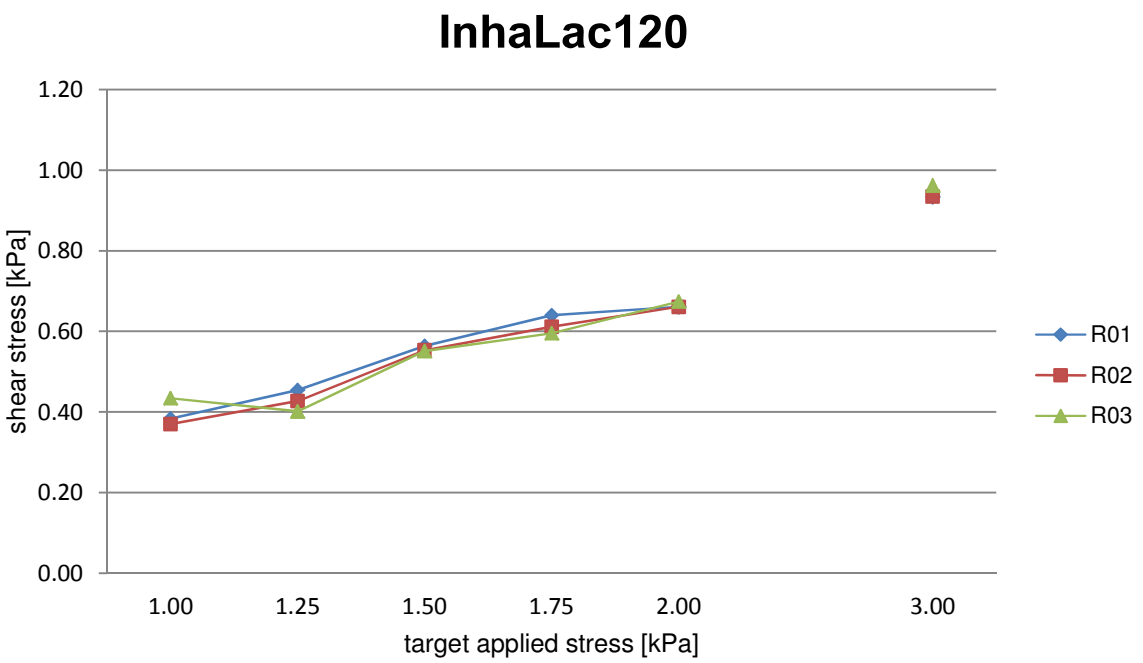

Figure 42: InhaLac120 yield loci.

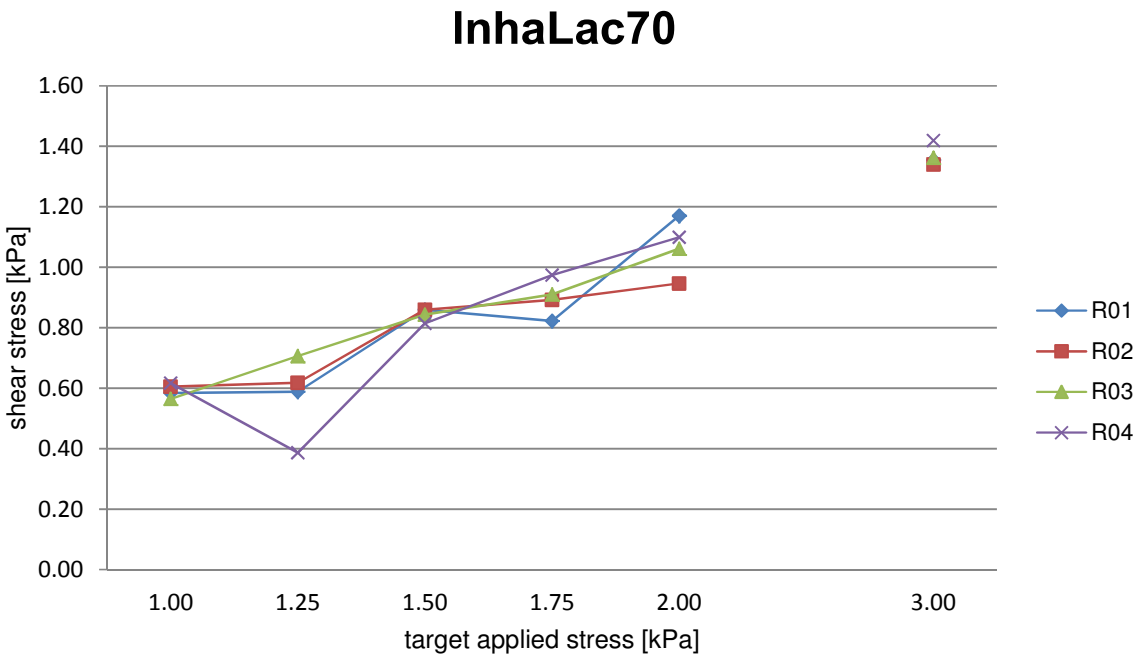

Figure 43: InhaLac70 yield loci.

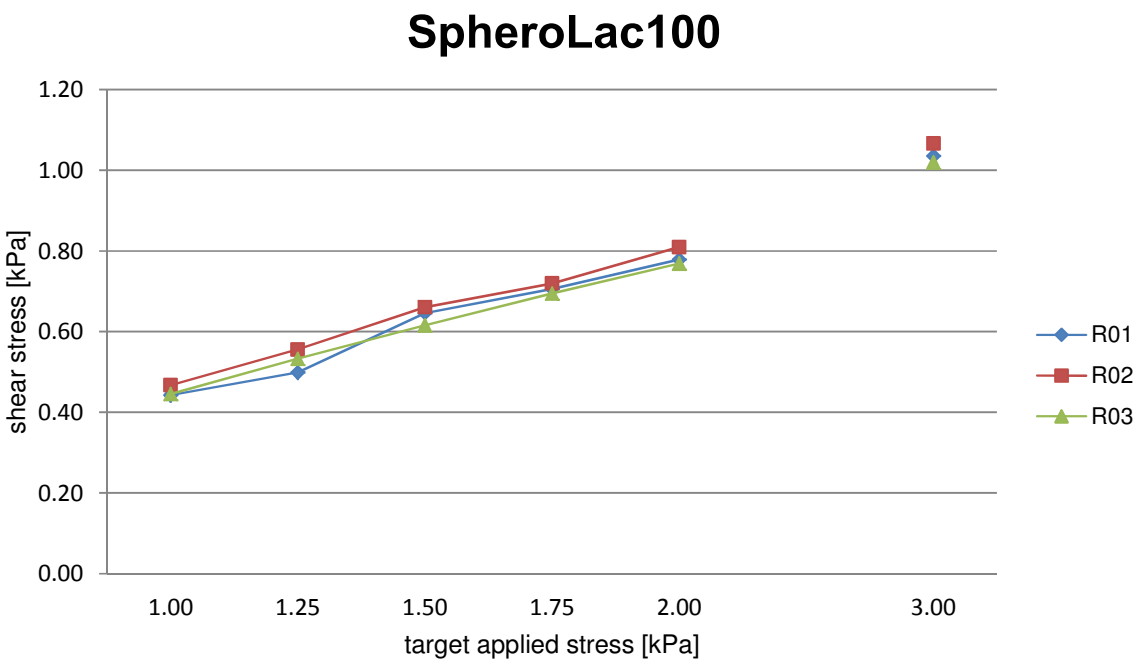

Figure 44: SpheroLac100 yield loci.

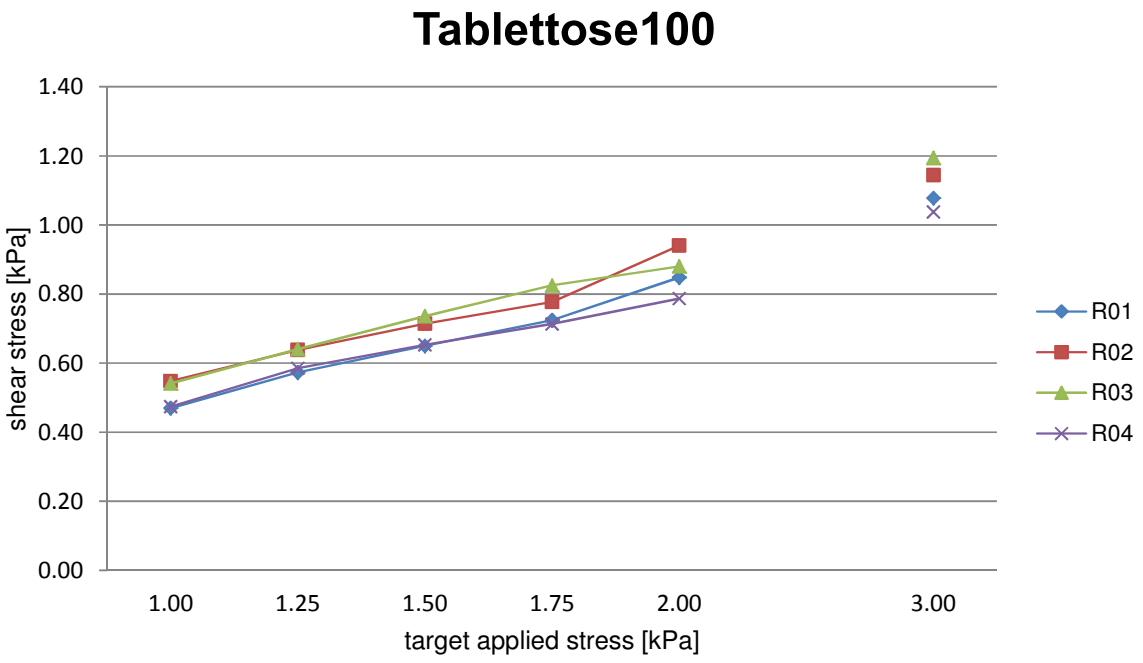

Figure 45: Tablettose100 yield loci.

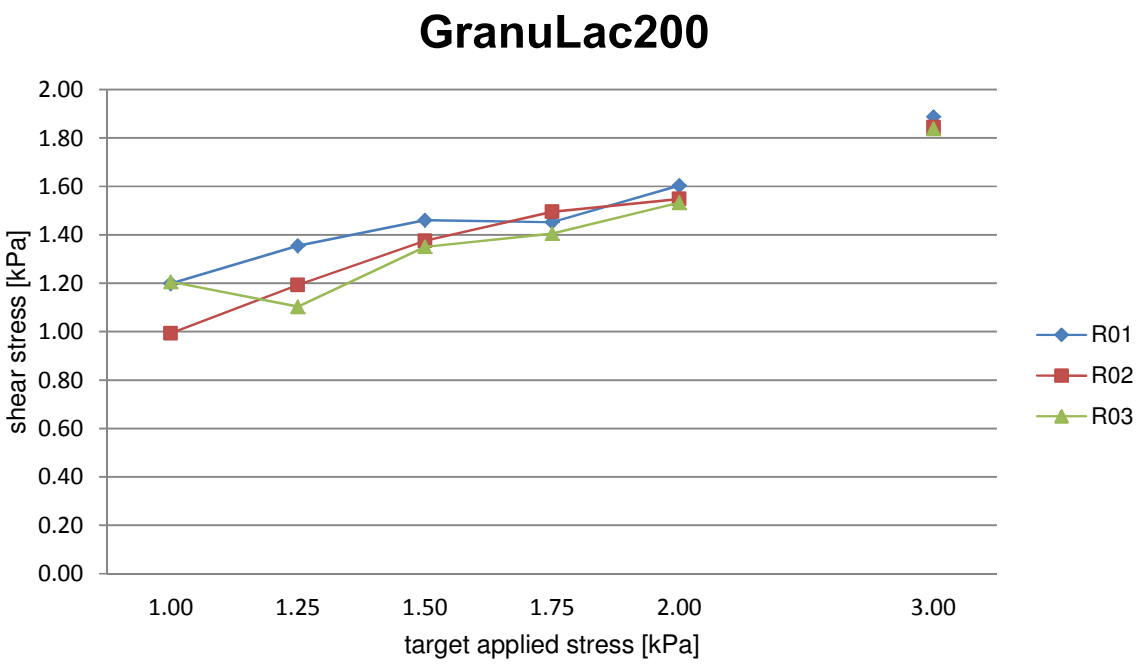

Figure 46: GranuLac200 yield loci.

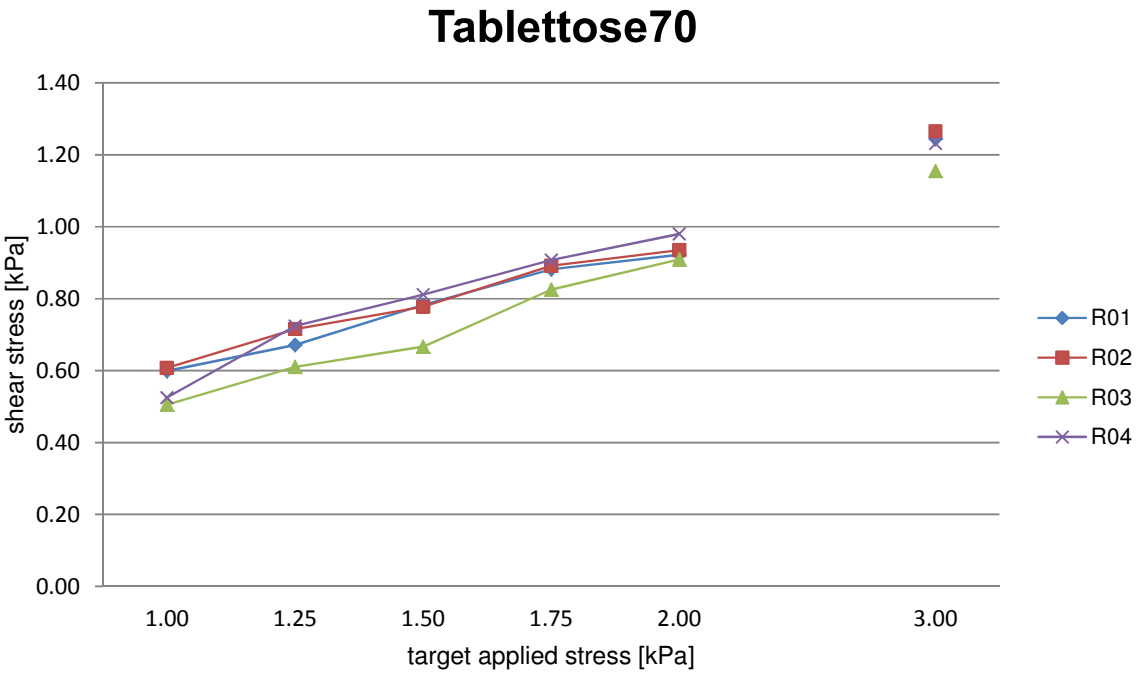

Figure 47: Tablettose70 yield loci.

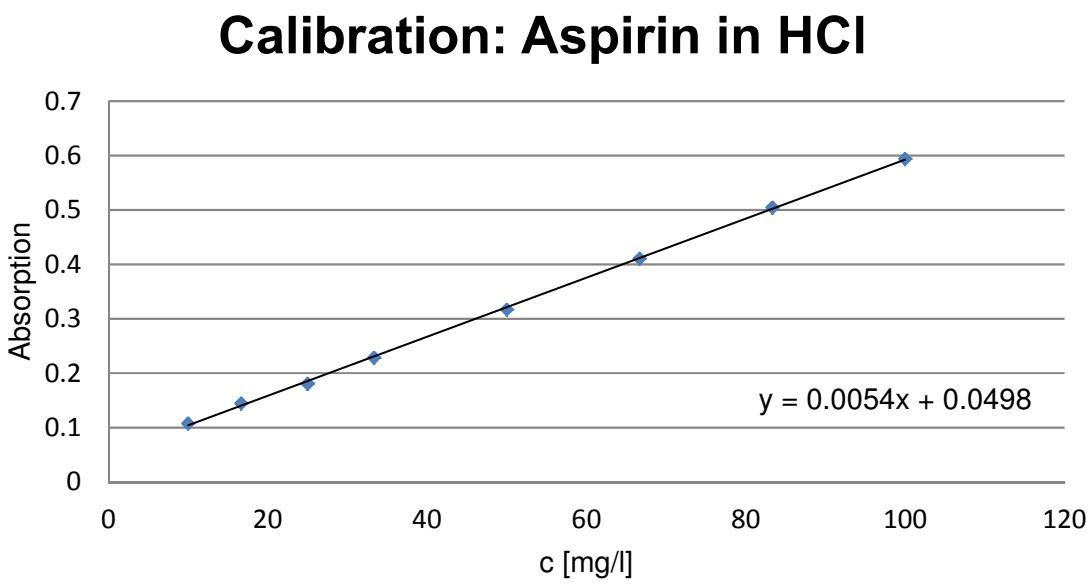

Figure 48: Aspirin calibration in hydrochloric acid solution and linear regression used in the calculations.

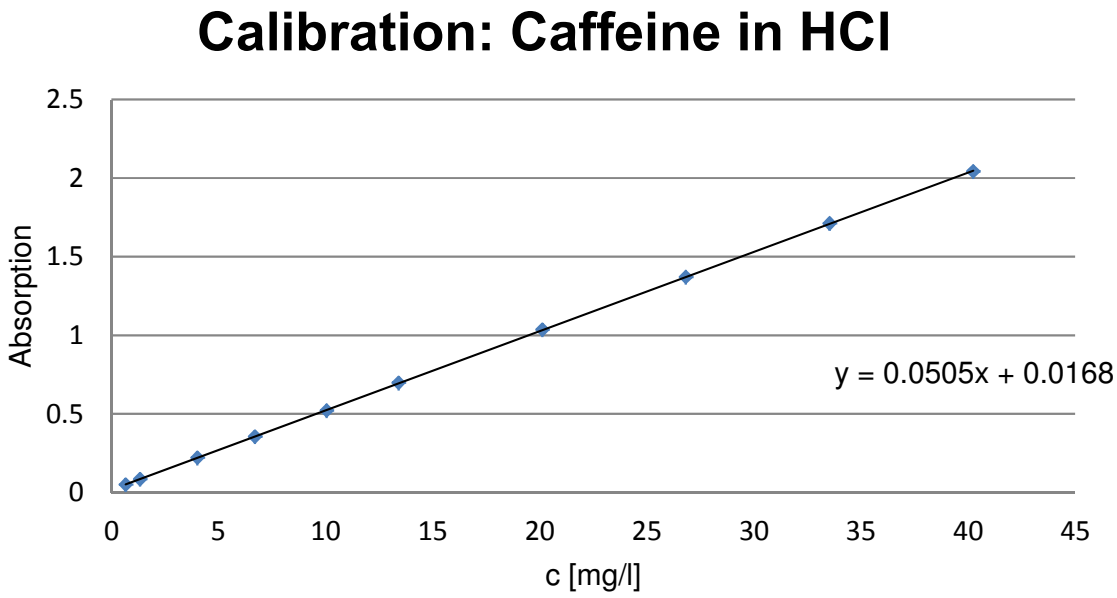

Figure 49: Caffeine calibration in hydrochloric acid solution and linear regression used in the calculations.

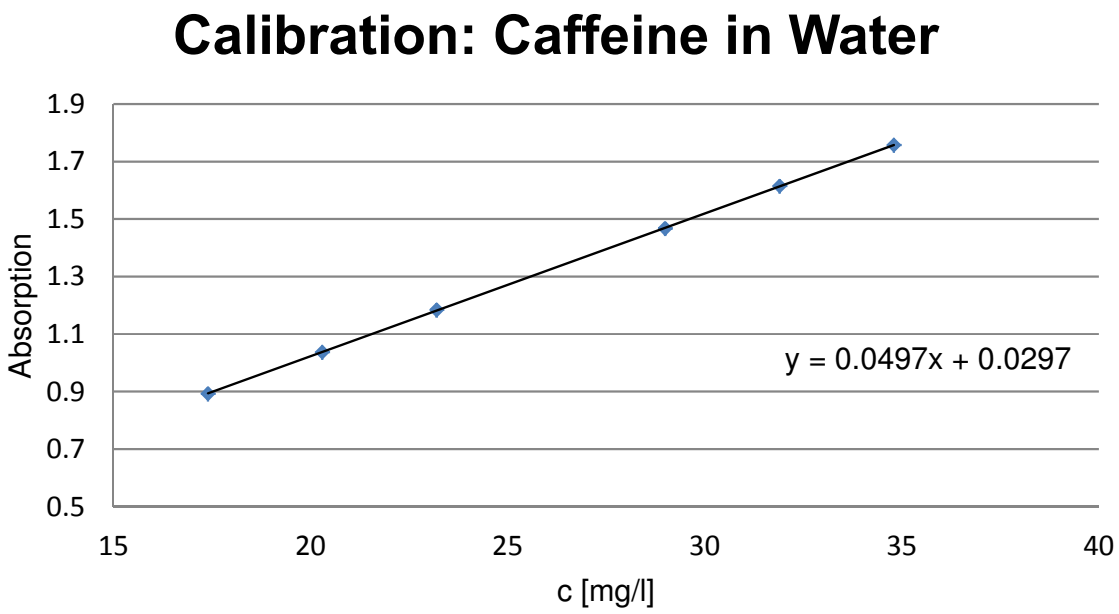

Figure 50: Caffeine calibration in distilled water and linear regression used in the calculations.

[1] Atkins P., de Paula J., *Physical Chemistry,* **2006,** 4th edition
[2] ElMasry G., Sun S., *Hyperspectral Imaging for Food Quality Analysis and Control*, **2010**
[3] Gendrin C., Roggo Y., Collet C., *Journal of Pharmaceutical and Biomedical Analysis,* **2008**, *48*, 533-553
[4] Jamrógiewicz M., *Journal of Pharmaceutical and Biomedical Analysis*, **2012**, *66*, 1-10
[5] Siesler H., Ozaki Y., Kawata S., Heise H., *Near-Infrared Spectroscopy*, **2002**
[6] Roggo Y., Chalus P., Maurer L., Lema-Martinez C., Edmont A., Jent N., *Journal of Pharmaceutical and Biomedical Analysis,* **2007,** *44,* 683-700
[7] Reich G., *Advanced Drug Delivery Reviews,* **2005**, *57*, 1109-1143
[8] Lyon R., Lester D., Lewis E., Lee E., Yu L., Jefferson E., Hussain A., *AAPS Pharm Sci Tech*, **2002**, 3 (3), article 17
[9] Quin J., *Hyperspectral Imaging for Food Quality Analysis and Control*, **2010**
[10] Short S., Cogdill R., Wildfong P., Drennen J., Anderson C., *Journal of Pharmaceutical Science,* **2009**, *98* (3), 1095-1109
[11] US Pharmacopoeia
[12] European Pharmacopoeia 5.0, *Dissolution test for solid dosage forms*, 228-230
[13] Tadley T., Carr G., *Pharmaceutical Formulation and Quality,* **2009**
[14] Hesse M., Meier H., Zeeh B., *Spectroscopic methods in organic chemistry,* **2005**, 7th edition
[15] Gottwald W., Heinrich K.H., *UV/VIS-Spektroskopie für Anwender*, **1998**